

CLASSIFICATION OF 2-NODE EXCITATORY-INHIBITORY NETWORKS

MANUELA AGUIAR, ANA DIAS, AND IAN STEWART

ABSTRACT. We classify connected 2-node excitatory-inhibitory networks under various conditions. We assume that, as well as for connections, there are two distinct node-types, excitatory and inhibitory. In our classification we consider four different types of excitatory-inhibitory networks: restricted, partially restricted, unrestricted and completely unrestricted. For each type we give two different classifications. Using results on ODE-equivalence and minimality, we classify the ODE-classes and present a minimal representative for each ODE-class. We also classify all the networks with valence ≤ 2 . These classifications are up to renumbering of nodes and the interchange of ‘excitatory’ and ‘inhibitory’ on nodes and arrows. These classifications constitute a first step towards analysing dynamics and bifurcations of excitatory-inhibitory networks. The results have potential applications to biological network models, especially neuronal networks, gene regulatory networks, and synthetic gene networks.

1. INTRODUCTION

In many biological networks there is a key distinction between *excitatory* and *inhibitory* connections. These terms are common in neuroscience; in genetics the corresponding connections are usually called *activators* and *repressors*. For simplicity we adopt the excitatory/inhibitory terminology in this paper.

A connection from node i to node j is excitatory when activation of node i makes node j more likely to become active. A connection is inhibitory if activation of node i makes node j less likely to become active. The precise level of activity is determined by the detailed dynamics of the nodes and arrows; in particular, by the strength of the connection. Examples where this distinction is of central importance are networks of neurons, such as the connectome of an organism (Hagmann [29], Sporns *et al.* [49]) and gene regulatory networks (GRNs), Liu *et al.* [39].

Date: March 6, 2024.

2020 Mathematics Subject Classification. Primary: 92C42, 37N25, 37C20; Secondary: 92B20 .

Key words and phrases. excitatory-inhibitory network, excitatory and inhibitory connections, ODE-equivalence .

A mathematical framework for understanding collective dynamics on coupled networks, such as synchronization and synchrony-breaking or synchrony-preserving bifurcations, is supplied by the theory of *(coupled cell) networks* and corresponding *network dynamical systems* or *admissible ODEs*, see Golubitsky *et al.* [50, 24, 19, 22] and Field [15]. In this formalism, nodes and connections (‘arrows’) are assigned ‘types’, which constrain the class of admissible ODEs. For classification purposes we distinguish excitatory nodes from inhibitory ones by assigning them different types, but make no other assumptions. See Section 1.4. The aim of this paper is to classify 2-node networks with two different types of connection, under a variety of extra conditions, summarized in Table 1. A companion paper [6] builds on these results to extend the classifications to 3-node excitatory-inhibitory networks.

In neuronal networks, as a general (though not universal) rule, the type of connection is determined by its tail node. In other words, nodes (as well as connections) are of two types, *excitatory* and *inhibitory*. Excitatory nodes output excitatory signals and inhibitory nodes output inhibitory signals. This condition does not apply to GRNs: a single node can have both excitatory and inhibitory outputs.

1.1. Motivation from Previous Work. Mathematical models of GRNs and results on robust synchronization, based on the existing theoretical results in the above network formalism, have been obtained by Aguiar, Dias and Ruan [4]. A related theory of homeostasis in network dynamics has been developed by Golubitsky *et al.* [20, 21, 23, 25] and applied to GRNs by Antoneli *et al.* [7]. Synchrony-breaking bifurcations for six small, basic genetic circuits are studied in Makse *et al.* [41].

Even when the full network is large and complex, many subnetworks have been identified that enable specific, useful functions within that network. These subnetworks, often called *motifs*, are small subnetworks with a topology that occurs with significantly higher frequency than in randomized networks, Milo *et al.* [43]. Tyson and Novák [52] have classified 2- and 3-node motifs in biochemical reaction networks. They analyze the dynamics of these motifs and provide evidence that they can carry out specific functions. Singhania and Tyson [47] point out that there are many examples of *near-perfect adaptive responses* in the physiology of living cells, which corresponds to the transiently dynamics response of a system to a change in an environmental signal and then returning near perfectly to its pre-signal state, even in the continued presence of the signal. Using an evolutionary search procedure, [47] addresses the underlying molecular bases of such behavior. More precisely, it examines a wide class of molecular interaction 3-node motif networks for their potential to exhibit near-perfect adaptation.

Leifer *et al.* [37] and Morone *et al.* [44] argue that in order to be a functional biological building block, a small subnetwork should not just occur unusually often, but it should offer computational repertoires analogous to electronic circuits. This

idea has been explored in synthetic biology, showing that small engineered GRNs can perform logical computations, Dalchau *et al.* [11]. An example is the toggle switch, which can be made to switch between two coexisting stable states by providing suitable inputs [8, 18, 33, 34].

Another example occurs in Elowitz and Leibler [14], who assembled a synthetic oscillatory network in *Escherichia coli* from three transcriptional repressor systems, naming it the *repressilator*. They observed periodic oscillations with a period of several hours. For simplicity, they first analyze an idealized model in which all three repressors have the same dynamics, so the equations are symmetric under the cyclic group \mathbb{Z}_3 of order 3. Simulations of oscillatory motion produced a discrete rotating wave with successive $\frac{1}{3}$ -period phase shifts. Using methods of network dynamics, this state is typical of \mathbb{Z}_3 -symmetric systems, and often occurs via symmetry-breaking Hopf bifurcation, Golubitsky and Stewart [22]. A stochastic version in [14] produced oscillations of different and variable amplitudes, but with approximately the same $\frac{1}{3}$ -period phase shifts.

Several other standard synthetic genetic oscillators, whose structure is that of a small network, are surveyed in Purcell *et al.* [46]. They include:

(i) The *Goodwin oscillator*, Goodwin [26], which comprises a single gene that represses itself.

(ii) *Amplified negative feedback oscillators* have been studied by several authors, using different mathematical models. Guantes and Poyatos [28] explain oscillation as a saddle-node bifurcation on an invariant circle (SNIC). Conrad *et al.* [10] obtain oscillations from a subcritical Hopf bifurcation. Atkinson *et al.* [8] also use Hopf bifurcation.

(iii) The *Fussenegger oscillator* goes back to Tigges *et al.* [51]. It comprises two genes, with both sense and antisense transcription occurring from one of them. This creates a delay in the feedback loop, enhancing the ability to oscillate

(iv) The *Smolen oscillator*, Smolen *et al.* [48], comprises two genes. One promotes its own transcription and that of the other gene, while the second represses its own transcription and that of the first gene. Oscillations were first demonstrated mathematically in Hasty *et al.* [30] using a simple model, and shown to arise from either a supercritical or subcritical Hopf bifurcation.

(v) In a *variable link oscillator* one gene regulates itself, and also regulates a second gene through a variable promoter. The second gene causes repression via a protease acting on the product of the first gene. An ODE model is studied in Hasty *et al.* [31].

(vi) The *metabolator*, Fung *et al.* [16], is the first biological oscillator reported in the literature using metabolites as a core component.

1.2. Motifs in *Escherichia coli* GRN. As further motivation, Figure 1 shows eight 3-node motifs from the gene regulatory network of *Escherichia coli*, an organism

whose genetic regulatory network, compiled by RegulonDB, has been characterised in considerable detail [17]. The main point of the figure is to illustrate the presence of nontrivial 3-node motifs in real biological networks, but they also illustrate features of the mathematical classification developed in this paper. We discuss each motif briefly.

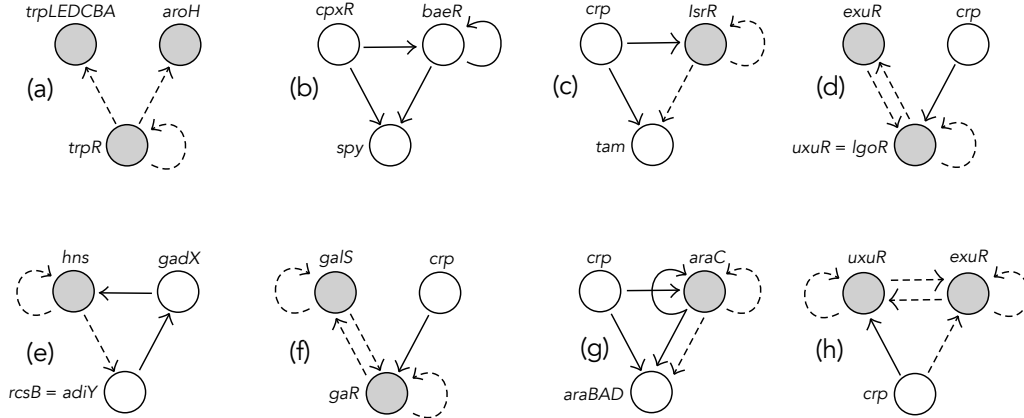


FIGURE 1. Eight 3-node motifs realised in *E. coli*.

(a) Autoregulation loop involved in biosynthesis of tryptophan, regulated by *trpR* [27], which represses itself, the gene *aroH*, and the *trpLEDCBA* operon, which codes for the enzymes of the tryptophan biosynthesis pathway. From [42].

(b) Example of a SAT-Feed-Forward-Fiber network. From [37] Fig.1 E.

(c) Example of an UNSAT-Feed-Forward-Fiber network. From [37] Fig.2 F.

(d) Example of a 2-FF network showing quotient by synchrony of genes *uxuR* and *IgoR* in a 4-node network in *E.coli*. From [44] Fig. 3B.

(e) Example of a 3-FF network showing quotient by synchrony of genes *rcsB* and *adiY* in a 4-node network in *E.coli*. From [44] Fig. 3B.

(f) Example of a a network where a node feeds forward into one node of a toggle-switch. From [40].

(g) In the sugar utilisation transcriptional system [24], the arabinose metabolism [25] involves the regulation of the *araBAD* operon (composed of genes *araB*, *araA*, and *araD*) by two transcription factors *AraC* and *CRP* expressed by genes *araC* and *crp*, respectively. From [45].

(h) Example of a network where a node feeds forward into both nodes of a toggle-switch. From [45].

Networks (a) and (b) have arrows (and nodes) of a single type. Networks (c),(d),(e), and (f) are what we call REI networks in Definition 2.3 below; that is, a given node

outputs only one type of arrow. Networks (g) and (h) are UEI networks: some node outputs arrows of both types.

1.3. Classification. Given this degree of interest in small GRNs and their dynamics and bifurcations, it is of interest to formalize the structure of excitatory-inhibitory (EI) networks and to investigate small examples systematically. We aim to classify small EI networks under certain conditions. In this paper we classify 2-node EI networks. These results are extended to the 3-node case in [6]. These classifications can be viewed as a preparatory step towards a systematic analysis of dynamics and bifurcations in such networks.

We work in the network formalism of [50, 24, 22], in which nodes (previously called cells) and arrows (connections, directed edges) are partitioned into one or more types. The dynamics of the network respects both its topology and the distinction between different types of node or arrow. Such systems of ordinary differential equations (ODEs) are said to be *admissible* for the network.

The classification of regular 3-node networks, that is, with only one node and arrow type and where every node receives one or two arrows, can be found in [38], along with the classification of all codimension one steady-state and Hopf bifurcations from a synchronous equilibria in these networks.

Our classifications are modelled on that analysis. However, [38] also considers the dynamics and bifurcations, topics for future work on EI networks. Similar classifications have been carried out for regular 4-node networks by Kamei [32], 3-node fully inhomogeneous networks [22, Section 4.4] and networks with asymmetric inputs by Aguiar, Dias and Soares [5]. Nevertheless, the special structure of excitatory-inhibitory networks has not previously been addressed in a systematic manner.

1.4. Remarks on Excitation and Inhibition. The general formalism of [50, 24, 22] does not assign a meaning to the terms ‘excitatory’ or ‘inhibitory’ when applied to a specific arrow in a network diagram. It does, however, distinguish different *types* of connections (arrows), which is sufficient for classification purposes. One reason for this approach is that the formalism is designed to apply to all ODE models with network structure, in many of which notions of excitation and inhibition are not relevant. Another is that couplings are assumed to be determined by general nonlinear functions, whereas excitation/inhibition is most natural for linear couplings, see below.

However, the correspondence with biological notions of excitation and inhibition appears in the general formalism when we introduce an important feature: the *dynamics* of an admissible ODE. It is then possible to define excitation/inhibition relative to a specific *solution* of the ODE, such as an equilibrium or periodic orbit. This definition usually agrees with the terms as used in standard biological models.

In general, an admissible ODE assigns a variable x_i to each node i , representing its dynamic state, and takes the form

$$\dot{x}_i = f_i(x_i; x_{i_1}, \dots, x_{i_m}),$$

where i indexes the nodes and i_1, \dots, i_m run through the tail nodes of all input arrows to node i . Moreover, if nodes i, j have the same node-type and the same number of input arrows of each arrow-type, we require $f_i = f_j$.

Definition 1.1. Assume for simplicity that x^* is an equilibrium. Then the k th input arrow to node i is:

$$(1.1) \quad \begin{aligned} & \text{excitatory at } x^* && \text{if } \partial_k f_i|_{x^*} > 0, \\ & \text{inhibitory at } x^* && \text{if } \partial_k f_i|_{x^*} < 0. \end{aligned}$$

Here $\partial_k f_i$ is the partial derivative of f_i with respect to the k th variable, excluding the first variable x_i which represents the state of the node concerned. (We do not write these in the more familiar form $\frac{\partial f_i}{\partial x_{i_k}}$ because the same variable x_{i_k} may appear for different values of k , in which case that notation is ambiguous.) \diamond

In many common models, couplings are linear, so that

$$(1.2) \quad \dot{x}_i = f_i(x_i) + \alpha_1 x_{i_1} + \dots + \alpha_m x_{i_m}.$$

with only f_i nonlinear. Models of this kind go back at least to Kuramoto [35, 36]. Here the coefficients α_k are often called *connection strengths* or *weights*. Now arrow k is excitatory (for any solution) if $\alpha_k > 0$, and inhibitory if $\alpha_k < 0$. Therefore (1.1) is in agreement with standard terminology for such models.

These considerations do not affect the classifications in this paper, or the lists of admissible ODEs. However, they can be vital when considering dynamics and bifurcations.

1.5. Summary of Paper and Main Results. In this paper we define four different types of EI networks: REI, PEI, UEI, and CEI, see Definition 2.3. These definitions form the basis of this paper and the companion [6]. In both papers we classify networks of these types under various assumptions. We also derive subsidiary classifications under the stronger relation of ODE-equivalence, where two networks are ODE-equivalent if they have the same space of admissible ODEs. To organise and summarise these results, Table 1 lists the main classifications obtained in this paper, with columns for the bounds on the valence, type of network, number of networks in the classification, plus references to associated Figures, Theorems, and lists of admissible ODEs. Even in the 2-node case, we find a rich variety of networks. The 3-node case, which is more complicated, makes use of the 2-node results.

Section 2 discusses classes of excitatory-inhibitory (EI) networks from the point of view of the general network formalism of [50, 24, 22]. In this formalism the

network type	number of networks	figure	theorem	admissible ODEs
REI	∞	Figure 4 (left)	Proposition 3.1	(3.4)
REI (ODE)	2	Figure 5	Proposition 3.3	Table 2
REI val ≤ 2	15 2 ODE-classes	Figure 6 Figure 5	Proposition 3.4	Table 3 Table 2
PEI	∞	Figure 7	Proposition 3.1	(3.4)
PEI (ODE)	∞	Figure 8	Proposition 3.7	Table 4
PEI val ≤ 2	15 9 ODE-classes	Figure 6 nodes same type Figure 9	Proposition 3.8	Table 3 Table 5
UEI (ODE)	∞	Figure 11	Proposition 3.10	Table 6
UEI (ODE) val ≤ 2	4	Figure 12	Proposition 3.11	Table 7
UEI val ≤ 2	53 4 ODE-classes	Figures 6 and 13 Figure 12	Proposition 3.12	Tables 3 and 8 Table 7
CEI	∞	Figure 14	Proposition 3.15	(3.9)
CEI (ODE)	∞	—	Proposition 3.16	—
CEI val ≤ 2	53 21 ODE-classes	Figures 6 and 13 nodes same type Figures 9 and 15	Proposition 3.17	Tables 3 and 8 Tables 5 and 9

TABLE 1. List of classifications of connected 2-node EI networks and their locations. (ODE): ODE-equivalence classes. val: valence.

two arrow-types are different, but the \pm nature of excitation/inhibition is defined relative to a given dynamical state by (1.1). We distinguish excitatory nodes from inhibitory ones, giving two distinct node-types. It is also possible to identify these node-types subject to conditions on their output arrows. Doing so creates extra synchrony patterns as in [37, 41, 44], but we do not discuss these patterns here. Subsection 2.1 gives formal definitions of four types of excitatory-inhibitory networks, ‘restricted’ (REI), ‘partially restricted’ (PEI), ‘unrestricted’ (UEI), and ‘completely unrestricted’ (CEI). Subsection 2.2 defines the class of admissible ODEs associated with an EI network, using the Smolen oscillator as a simple example. Adjacency matrices are also discussed. Subsection 2.3 defines balanced colourings (also called fibration symmetries) and the associated quotient networks.

Section 3 classifies 2-node EI networks under various conditions. Corresponding admissible ODEs are listed. Subsections 3.1-3.3 are dedicated to the classification of connected 2-node REI networks. In Subsection 3.2, the classification is done up to ODE-equivalence and in Subsection 3.3 for REI networks of valence ≤ 2 . Subsections 3.4-3.6 consider the classification of connected 2-node PEI networks. In Subsection 3.5, the classification is done up to ODE-equivalence and in Subsection 3.6 is for 2-node PEI networks of valence ≤ 2 . Subsections 3.7-3.9 address the classification of connected 2-node UEI networks, where Subsection 3.8 classifies up to ODE-equivalence and Subsection 3.9 lists the 2-node UEI networks of valence ≤ 2 .

Finally, Subsections 3.10-3.12 classify connected 2-node CEI networks, where the classification in Subsection 3.11 is done up to ODE-equivalence and the classification in Subsection 3.12 is of the networks of valence ≤ 2 .

2. CLASSES OF EXCITATORY-INHIBITORY NETWORKS

We use the network formalism of [50, 24], modified as in [22] to remove the condition that arrows of the same type have heads of the same type and tails of the same type. Instead, we separate the roles of node equivalence (formerly cell equivalence) and state equivalence (a consequence of the constraints on admissible maps and ODEs). Nodes are state-equivalent if they have the same state space in a canonical manner. Intuitively, they are node equivalent if they have the same ‘internal dynamic’. This change broadens the range of networks without affecting the main theorems or their proofs. It is also more natural for the networks considered in this paper.

Remarks 2.1. (i) Technically, the node-type can be considered as an arrow-type for a distinguished ‘internal arrow’. It constrains the admissible ODEs *only* when two nodes c, d of the same node-type are input equivalent. Otherwise, equal node types have no dynamic implications.

(ii) This convention differs considerably from that of many models, where each node or arrow contributes a specific *term* to the model ODE. The reasoning behind it is explained in [22, Sections 9.5, 9.8]. A key point is that nodes can synchronize robustly only when they have the same node type *and* have isomorphic input sets. If the input sets of nodes c, d are not isomorphic, assigning them the same node-type is redundant and does not constrain the admissible ODEs. Node-types can be redefined to remove these redundancies.

(iii) In many areas of science, the zero state $x_i = 0$ has a special significance. For example, in a biochemical or gene regulatory network, the concentration of a molecule is always ≥ 0 , and a concentration of 0 implies its absence. In a neuronal network, a voltage of 0 also has a clear physical meaning. In many applications it is assumed that the model ODE has the form $\dot{x} = F(x)$ where $F(0) = 0$, implying the existence of a fully synchronized state in which $x = (0, 0, \dots, 0)$. This state exists even when nodes are not input isomorphic.

(iv) However, in other areas of application there is nothing special about the value 0. The general formalism therefore assigns no special significance to the zero state, and a fully synchronized state may not exist unless the network is homogeneous.

(v) Similar remarks apply to weighted networks, and to network models of the form (1.2).

As remarked in Section 1.4, on a formal level the distinction between excitatory arrows and inhibitory ones reduces to having two different arrow-types A^E, A^I . We

use *only* two arrow-types, which corresponds to a standard simplified modelling assumption: all excitatory arrows are identical and all inhibitory arrows are identical. Without this assumption the lists of networks become much larger.

Node-types pose an additional problem. In some areas of biology, notably neuroscience, a given node cannot output both an excitatory arrow and an inhibitory one. In effect, there are two distinct node-types N^E, N^I . This assumption leads to the class of *restricted* EI-networks (REI).

However, this restriction is not universal; for example it often fails in GRNs. Keeping two node-types but removing the restriction on outputs gives the class of *unrestricted* EI-networks (UEI).

Remark 2.2. Other classes of EI networks are also of interest, in particular in connection with a feature of network dynamics that is important in both theory and applications: synchrony. Two nodes are *synchronous* if they have identical time series for some solution of the model equations. Here we mention synchrony only in passing, but some discussion is in order because of its importance. A synchronous state is *robust* if it is determined by a subspace that is invariant under all admissible maps. Every robustly synchronous state corresponds to a *balanced colouring* of the nodes, see Section 2.3. This determines a *synchrony pattern* whose *synchrony subspace* is flow-invariant for all admissible ODEs. In consequence, nodes with different node-types cannot synchronise robustly.

In this paper we assume that there are two distinct node-types: N^E (excitatory) and N^I (inhibitory). Since robustly synchronous nodes must be input-isomorphic, an N^E node cannot synchronise robustly with an N^I node. This constraint reduces the range of possible synchrony patterns. From this viewpoint, REI and UEI networks are never homogeneous (all nodes cannot synchronize simultaneously and robustly). For example, the Smolen network of Figure 2 cannot have a nontrivial synchrony pattern. (In the trivial pattern, each node has a different colour. The trivial colouring is obviously balanced.) Another term for the same idea, discovered independently in a different context, is *fibration symmetry*; see Boldi and Vigna [9] and DeVille and Lerman [12].

In contrast, the networks studied in [37, 41, 44] can have more synchrony patterns and, in particular, a total synchrony pattern where all nodes synchronize simultaneously and robustly. This happens because, in effect, the two node-types N^E, N^I are considered to be the same. This assumption is reasonable in neuronal networks, where *activation* of a neuron either excites or inhibits another neuron. This suggests that the difference lies in the outputs, or in how a node receiving the output responds to that signal, but not in the internal dynamics of the neuron. With this assumption, the Smolen network can synchronize robustly.

In the REI case, consider the modification where the two node-types are identified but the restriction that no node outputs arrows of both types A^E, A^I is retained. We call these *partially restricted* EI-networks (PEI). The same modification can be done in the UEI case, and amounts to giving all nodes the same type without arrow-type restrictions. We call these *completely unrestricted* EI-networks (CEI). \diamond

For PEI and CEI networks all nodes have the same node-type, which implies a change to the admissible ODEs by imposing further constraints on the component functions, and so extra synchrony patterns can arise.

2.1. Formal Definitions. We define four classes of *excitatory-inhibitory networks*.

Definition 2.3. Consider the following four conditions on a network \mathcal{G} :

- (a) There are two distinct node-types, N^E and N^I .
- (b) There are two distinct arrow-types, A^E and A^I .
- (c) If $e \in A^E$ then $\mathcal{T}(e) \in N^E$.
- (d) If $e \in A^I$ then $\mathcal{T}(e) \in N^I$,

where $\mathcal{T}(e)$ indicates the tail node of arrow e .

Then:

\mathcal{G} is a *restricted excitatory-inhibitory network* (REI network) if it satisfies conditions (a), (b), (c) and (d).

\mathcal{G} is an *unrestricted excitatory-inhibitory network* (UEI network) if it satisfies conditions (a) and (b).

\mathcal{G} is a *partially restricted excitatory-inhibitory network* (PEI network) if the node-types N^E and N^I are identified (so (a) fails to apply) and it satisfies condition (b). Conditions (c) and (d) fail to apply, but each node outputs only one type of arrow.

\mathcal{G} is a *completely unrestricted excitatory-inhibitory network* (CEI network) if the node-types N^E and N^I are identified (so (a) fails to apply) and it satisfies condition (b). Conditions (c) and (d) fail to apply and nodes can output the two types of arrow. \diamond

Remarks 2.4. (i) REI networks are, in particular, UEI networks and PEI networks are, in particular, CEI networks.

(ii) A PEI network has only one node-type and each node outputs arrows of only one type, but there are still two distinct arrow-types.

(iii) CEI networks employ the convention of [37, 44], in which there is one node-type but two distinct arrow-types. Each node can output arrows of either arrow-type. This modification seems inappropriate for neuronal networks, where excitatory neurons have different internal dynamics from inhibitory ones and networks are REI, but it can be appropriate for GRNs.

Conventions. The following conventions are used throughout the paper without further mention, except as an occasional reminder for clarity.

(a) We represent type N^E nodes by white circles and type N^I nodes by grey circles. Type A^E arrows are solid and type A^I arrows are dashed. (Various other conventions for excitatory/inhibitory arrows are found in the literature; this one is chosen for convenience.)

(b) All classifications are stated up to *renumbering* of nodes and *duality*; that is, interchange of ‘excitatory’ and ‘inhibitory’ on nodes and arrows: $N^E \leftrightarrow N^I$ and $A^E \leftrightarrow A^I$. \diamond

Definition 2.5. (a) Given a node i , denote the set of excitatory arrows directed to i by $I^E(i)$ and the set of inhibitory arrows directed to i by $I^I(i)$. We call $I^E(i)$ and $I^I(i)$ the *excitatory* and *inhibitory input sets* of i , respectively. The *input set* of i is then $I(i) = I^E(i) \cup I^I(i)$. The *valence (degree, in-degree)* of i is the cardinality $\#I(i)$ of $I(i)$.

(b) Two nodes i and j are *input equivalent* if they have the same node-type and there is an arrow-type preserving bijection between the corresponding input sets $I(i)$ and $I(j)$; that is, when $\#I^E(i) = \#I^E(j)$ and $\#I^I(i) = \#I^I(j)$. We write $i \sim_I j$. The relation \sim_I is an equivalence relation, which partitions the set of nodes into disjoint *input classes*.

(c) A network in which all nodes are input equivalent is *homogeneous*. Otherwise, it is *inhomogeneous*. \diamond

Remarks 2.6. (i) The definition of synchrony in [22, 24, 50] implies that synchronous nodes must be input equivalent. Thus for EI networks, nodes of type N^E cannot synchronize with nodes of type N^I as, by Definition 2.5 (b), nodes of different types are not input equivalent. \diamond

(ii) Every REI and UEI network has two distinct node-types, N^E and N^I . Thus REI and UEI networks are inhomogeneous.

(iii) Since PEI and CEI networks have nodes of the same type, there can be homogeneous PEI and CEI networks.

A network is *transitive* if there is a closed arrow-path containing every node. A non-transitive network is often said to be *feedforward*. This term is also used for a stronger property: the nodes can be given a partial ordering such that the tail node of any arrow is smaller in the ordering than its head node.

2.2. Admissible ODEs. The dynamic evolution of node variables x_i is governed by a system of ordinary differential equations, said to be admissible. The form of admissible ODEs for EI networks can be deduced from the general definition in [22, 24, 50], but for convenience we describe it explicitly. We assume in this paper that all nodes have the same state space, say $P = \mathbb{R}^m$ for some $m > 0$. By definition,

input equivalent nodes must have the same node-type. Moreover, for each node i in a given input class, the dynamics is governed by the same smooth function, say $f : P^{k+1} \rightarrow P$, evaluated at the node i and at the node tails of the n_e excitatory and the n_i inhibitory arrows targeting that node. For the special case of EI networks, we have:

Definition 2.7. A system of ODEs is *admissible* for an EI network if it has the form

$$\dot{x}_i = f_i \left(x_i^s; \overline{x_{i_1}^+}, \dots, \overline{x_{i_{n_e}}^+}; \overline{x_{i_{n_e+1}}^-}, \dots, \overline{x_{i_{n_e+n_i}}^-} \right)$$

where $x_i^s \in \{x_i, x_i^+, x_i^-\}$ and the overlines indicate that the function f_i is symmetric in the overlined variables. The node variables are indexed by i . The *multiset* of all tail nodes of input arrows is the union of two subsets: the multiset $\{i_1, \dots, i_{n_e}\}$ of all tail nodes of the excitatory input set of node i , and the multiset $\{i_{n_e+1}, \dots, i_{n_e+n_i}\}$ of all tail nodes of the inhibitory input set of node i . The functional notation converts these multisets into tuples of the corresponding variables. We use the superscripts $+$ and $-$, as a notation convention, to make the distinction between the input variables corresponding to tail nodes in the excitatory and in the inhibitory input sets, respectively. Analogously, when there are two distinct node-types N^E and N^I , we use the superscripts $+$ and $-$ to make the distinction between the state variable of excitatory and inhibitory nodes. Otherwise, no subscript is used.

Moreover, if nodes i, j are in the same input class then $f_i = f_j$. \diamond

Remarks 2.8. (i) *Multiple arrows* are permitted. That is, distinct arrows in $I^E(i)$ can have the same tail node, which is why we use multisets. The same goes for $I^I(i)$. (ii) *Self-loops* are also permitted. That is, a node can input an arrow to itself. In biology this is called *autoregulation*. \diamond

If nodes i and j are input equivalent then $\#I^E(i) = \#I^E(j)$ and $\#I^I(i) = \#I^I(j)$. Therefore, if there is an arrow in $I(i)$ of a certain arrow-type, then there is also an arrow in $I(j)$ of the same type. The evolution in time of node j is defined similarly to that of node i , using the same function f evaluated at x_j and at the corresponding node tails. The evolution of nodes in different input classes is governed by different functions f_i , one for each input class.

Example 2.9. The *Smolen oscillator* in Figure 2 is an REI network. Node 1 is type N^E and node 2 is type N^I . There are two type A^E arrows; one from 1 to itself and the other from 1 to 2. There are two type A^I arrows; one from 2 to itself and the other from 2 to 1.

Each node has excitatory and inhibitory input sets with cardinality 1. Both nodes are autoregulatory.

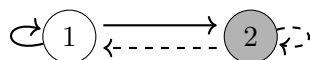


FIGURE 2. Smolen oscillator.

The node-types are different so this network is inhomogeneous. It is also *not* \mathbb{Z}_2 symmetric. Admissible ODEs are:

$$(2.3) \quad \begin{aligned} \dot{x}_1 &= f(x_1^+; x_1^+; x_2^-) \\ \dot{x}_2 &= g(x_2^-; x_1^+; x_2^-) \end{aligned} .$$

Here, $x_1^+, x_2^- \in P$ where P is the node state space and $f, g : P^3 \rightarrow P$ are smooth functions. This differs from the total phase space, which is P^2 ; such a difference occurs when there are multiple arrows or self-loops. With suitable dynamics modelling a GRN this network exhibits periodic oscillations, Purcell *et al.* [46]. \diamond

Remark 2.10. Considering the network in Example 2.9 with the alternative convention on node-types in PEI networks, all nodes are input equivalent, so the functions f and g are equal. Now there is a balanced colouring (fibration symmetry) in which $x_1 = x_2$ and the diagonal subspace $\Delta = \{x : x_1 = x_2\}$ is flow-invariant for any admissible ODE. Thus synchronous states can occur robustly. However, the Smolen oscillator network remains asymmetric because there are two arrow types. \diamond

We can represent an n -node network by its *adjacency matrix*, which is the $n \times n$ matrix $A = (a_{ij})$ such that a_{ij} is the number of arrows from node j to node i . Ordinarily, this representation could lose information, because it fails to distinguish the different arrow-types. However, conditions (c) and (d) of Definition 2.3 allow us to deduce the arrow-types for REI networks, provided we know the node-types of nodes i and j . The networks that are PEI, CEI, and UEI require two adjacency matrices, one for each arrow-type; see the next example.

Example 2.11. The adjacency matrix of the Smolen network in Figure 2 is

$$\begin{bmatrix} 1 & 1 \\ 1 & 1 \end{bmatrix} .$$

For some purposes, such as ODE-equivalence, we must distinguish node- and arrow-types and equip each with its own adjacency matrix. Here there are four:

$$\begin{aligned} \text{Node-type } N^E: & \begin{bmatrix} 1 & 0 \\ 0 & 0 \end{bmatrix}; & \text{Node-type } N^I: & \begin{bmatrix} 0 & 0 \\ 0 & 1 \end{bmatrix}; \\ \text{Arrow-type } A^E: & \begin{bmatrix} 1 & 0 \\ 1 & 0 \end{bmatrix}; & \text{Arrow-type } A^I: & \begin{bmatrix} 0 & 1 \\ 0 & 1 \end{bmatrix}. \end{aligned}$$

Alternatively, if we assume the Smolen network to be a PEI network (just one node-type), then there are three adjacency matrices:

$$\begin{aligned} \text{Node-type } N^E = N^I: & \begin{bmatrix} 1 & 0 \\ 0 & 1 \end{bmatrix}; \\ \text{Arrow-type } A^E: & \begin{bmatrix} 1 & 0 \\ 1 & 0 \end{bmatrix}; \quad \text{Arrow-type } A^I: \begin{bmatrix} 0 & 1 \\ 0 & 1 \end{bmatrix}. \end{aligned}$$

◇

Remark 2.12. (i) Different networks sometimes have the same set of admissible ODEs, for any choice of node state spaces, when their nodes are identified by a suitable bijection that preserves node state spaces. Such networks are *ODE-equivalent*, [13, 22, 24].

(ii) By Dias and Stewart [13, Theorem 7.1, Corollary 7.9], two networks with the same number of nodes are ODE-equivalent if and only if, for a suitable identification of nodes, they have the same vector spaces of *linear* admissible maps when node state spaces are \mathbb{R} . Equivalently, the adjacency matrices of all node- and arrow-types span the same space. Trivially, this remains true when restricting to the set of EI networks.

(iii) Following Aguiar and Dias [2, 3], given an ODE-class of EI networks, we can distinguish a subclass containing the EI networks in the ODE-class that have a minimal number of arrows. This is a *minimal subclass*. As an example, it is proved in [2] that the ODE-class of every homogeneous regular n -node network with only one arrow-type contains a unique minimal network. In general, the minimal class of an ODE-class need not be a singleton.

(iv) For REI networks, we saw that the node-types determine the arrow-types and the adjacency matrices naturally decompose into four blocks. The linear condition in (ii) preserves this decomposition, so two REI networks are ODE-equivalent if and only if these components are separately ODE-equivalent. Moreover, note that an ODE-class for an REI network always contains UEI networks that are not REI networks. Nevertheless, the methods of [2, 3] can easily be adapted to prove that there is an ODE-equivalence that preserves the REI structure for minimal subclasses. The corresponding issue for UEI networks is not true. For example, consider the 2-node UEI-network with arrow-type adjacency matrices

$$\text{Arrow-type } A^E: A_3 = \begin{bmatrix} 0 & 0 \\ 1 & 0 \end{bmatrix}; \quad \text{Arrow-type } A^I: A_4 = \begin{bmatrix} 0 & 1 \\ 1 & 0 \end{bmatrix}.$$

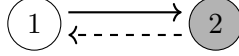


FIGURE 3. The minimal 2-node network ODE-equivalent to the Smolen oscillator in Figure 2.

Now observe that $A_4 - A_3 = \begin{bmatrix} 0 & 1 \\ 0 & 0 \end{bmatrix}$. Thus, the UEI-network is ODE-equivalent to the minimal REI-network with arrow-types adjacency matrices $\begin{bmatrix} 0 & 0 \\ 1 & 0 \end{bmatrix}$ and $\begin{bmatrix} 0 & 1 \\ 0 & 0 \end{bmatrix}$. \diamond

Example 2.13. In Sections 3.3 and 3.9, we determine the ODE-classes for the 2-node REI and UEI networks, respectively, with valence up to 2. As the ODE-classes for REI networks also contain UEI networks that are not REI networks, we have, as mentioned in Remark 3.14, that two of the ODE-classes for UEI networks coincide with the two ODE-classes for REI networks. The other two ODE-classes for UEI networks contain only UEI networks that are not REI networks. However, if we consider only the minimal ODE-classes, then for the REI case the classes contain only REI networks. For the UEI case, two of the classes contain only REI networks and the other two only UEI networks that are not REI networks. \diamond

Example 2.14. The REI network in Figure 3 is ODE-equivalent to the REI Smolen network in Figure 2 and it is minimal. Moreover, the admissible ODE (2.3) determines an arbitrary dynamical system in (x_1, x_2) . \diamond

2.3. Balanced Colourings and Quotient Networks. We specialise [50, Definition 6.4] to EI networks:

Definition 2.15. Consider an n -node EI network. Let \bowtie be an equivalence relation on the set $N^E \cup N^I$ of nodes, refining input equivalence. If $i \bowtie j$ then either $i, j \in N^E$ or $i, j \in N^I$. The relation \bowtie is *balanced* if, for every two nodes i, j such that $i \bowtie j$, there are arrow-type preserving bijections $\beta^E : I^E(i) \rightarrow I^E(j)$ and $\beta^I : I^I(i) \rightarrow I^I(j)$ such that if $e \in I^E(i)$ then $\mathcal{T}(e) \bowtie \mathcal{T}(\beta^E(e))$ and if $e \in I^I(i)$ then $\mathcal{T}(e) \bowtie \mathcal{T}(\beta^I(e))$. \diamond

Definition 2.16. Let \mathcal{G} be an EI network in which all node state spaces are P , and let \bowtie be a balanced equivalence relation on the set of nodes. Then the *polydiagonal (subspace)* $\Delta_{\bowtie} \subseteq P^n$ consists of all $x = (x_1, \dots, x_n)$ such that $i \bowtie j$ implies that $x_i = x_j$. The space Δ_{\bowtie} is also called a *synchrony subspace*. \diamond

By [22, Proposition 10.20] or [50, Theorem 6.5], a colouring \bowtie is balanced if and only if Δ_{\bowtie} is invariant under the flow of every linear network admissible ODE. This condition holds for any choice of node state spaces. Equivalently, \bowtie is balanced if and only if Δ_{\bowtie} is invariant under all adjacency matrices.

More generally, a vector subspace is a balanced polydiagonal, a synchrony subspace, if and only if it is invariant under any admissible ODE (including nonlinear ones): see [22, Theorem 10.21]. Synchrony subspaces therefore play a crucial role in the dynamics of admissible ODEs. See for example [1].

Following [24, Section 5], given an EI network \mathcal{G} and a balanced equivalence relation \bowtie with k classes, we can define the *quotient network* of \mathcal{G} by \bowtie . This is the k -node network whose nodes correspond to the \bowtie -equivalence classes, and whose arrows are the projections of those of \mathcal{G} , preserving arrow-type. It is variously denoted by \mathcal{G}/\bowtie , \mathcal{G}^{\bowtie} , or \mathcal{G}_{\bowtie} .

Trivially, we have:

Proposition 2.17. *For any EI network \mathcal{G} having a balanced equivalence relation \bowtie with k classes, the quotient of \mathcal{G} by \bowtie is a k -node EI network. Moreover, the quotient of \mathcal{G}/\bowtie is an REI (resp. UEI, CEI) network if and only if the network \mathcal{G} is REI (resp. UEI, CEI). \diamond*

Proof. Let \mathcal{G} be an EI network having a balanced equivalence relation \bowtie with k classes. By definition, \bowtie refines the input equivalence relation which refines that of node equivalence. Thus, the quotient \mathcal{G}/\bowtie is a REI (resp. UEI) network if and only if the network \mathcal{G} is REI (resp. UEI). Trivially, a quotient of a CEI network is a CEI network. \square

Remark 2.18. In the case of a PEI network, the quotient network is always a CEI network, but it might not be a PEI network. In a PEI network, if two nodes of the same colour output arrows of different type (one outputs excitatory arrows and the other inhibitory arrows) then in the quotient there is a node that outputs arrows of the two types, that is, the quotient is a CEI network. As an example, if \mathcal{G} is the Smolen oscillator in Figure 2 and we assume that the two nodes have the same type, that is, \mathcal{G} is a PEI network, then the equivalence relation $\bowtie = \{\{1, 2\}\}$ is balanced and \mathcal{G}/\bowtie is a CEI network. In fact, \mathcal{G}/\bowtie is the one-node network with two arrows (of different type) to itself and the synchrony space $\Delta_{\bowtie} = \{x : x_1 = x_2\}$ corresponds to the the diagonal subspace. Recall Example 2.9 and Remark 2.10. \diamond

Remark 2.19. By [22, Theorem 10.28] or [24, Theorem 5.2], every admissible ODE for \mathcal{G} restricted to Δ_{\bowtie} can be identified with an admissible ODE for the quotient \mathcal{G}/\bowtie . Moreover, every admissible ODE for the quotient \mathcal{G}/\bowtie can be identified with the restriction to Δ_{\bowtie} of an admissible ODE for \mathcal{G} . \diamond

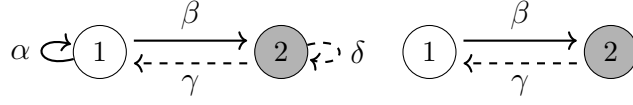


FIGURE 4. Two 2-node ODE-equivalent REI networks. Node 1 is excitatory, node 2 is inhibitory; the nonnegative integer arrow multiplicities are $\alpha, \beta, \gamma, \delta$. The network is connected when one of β or γ is nonzero.

3. CLASSIFICATION OF CONNECTED 2-NODE EXCITATORY-INHIBITORY NETWORKS

With these preliminaries out of the way, we now classify EI networks with two nodes. It is enough to classify connected networks, since components of a disconnected network have fewer nodes and the 1-node case is trivial.

We repeat Convention (b) in Section 2.1: all classifications are stated up to duality (interchange of the E and I types) and renumbering of nodes. We also consider ODE-equivalence. Based on this classification, we then list all the connected 2-node EI networks with valence at most 2 for any node. This condition eliminates most multiple arrows, which are uncommon (though possible) in real biological networks.

3.1. Connected 2-node REI Networks. We consider first 2-node REI networks. By duality, we assume that node 1 is excitatory and node 2 is inhibitory.

Proposition 3.1. *A 2-node connected REI network is the network of Figure 4 (left) for some choice of nonnegative integer arrow multiplicities $\alpha, \beta, \gamma, \delta$, where one of β or γ is nonzero. This network has admissible ODEs*

$$(3.4) \quad \begin{aligned} \dot{x}_1 &= f(x_1^+; \underbrace{x_1^+, \dots, x_1^+}_{\alpha}; \underbrace{x_2^-, \dots, x_2^-}_{\gamma}), \\ \dot{x}_2 &= g(x_2^-; \underbrace{x_1^+, \dots, x_1^+}_{\beta}; \underbrace{x_2^-, \dots, x_2^-}_{\delta}). \end{aligned}$$

Here $x_1^+, x_2^- \in \mathbb{R}^k$, so the total state space is \mathbb{R}^{2k} , and f and g are smooth functions invariant under permutation of the variables under each overline.

To simplify notation, temporarily omit the \pm superscripts, and define

$$(3.5) \quad p = (x_1, \underbrace{x_1, \dots, x_1}_\alpha, \underbrace{x_2, \dots, x_2}_\gamma); \quad q = (x_2, \underbrace{x_1, \dots, x_1}_\beta, \underbrace{x_2, \dots, x_2}_\delta);$$

$$a_1 = \frac{\partial f}{\partial x_1} \Big|_p; \quad b_1 = \frac{\partial f}{\partial x_2} \Big|_p; \quad c_1 = \frac{\partial f}{\partial x_{\alpha+2}} \Big|_p;$$

$$d_1 = \frac{\partial g}{\partial x_1} \Big|_q; \quad e_1 = \frac{\partial g}{\partial x_2} \Big|_q; \quad f_1 = \frac{\partial g}{\partial x_{\beta+2}} \Big|_q .$$

Then the linearization of (3.4) at (x_1, x_2) is the $2k \times 2k$ matrix

$$(3.6) \quad \begin{bmatrix} a_1 + \alpha b_1 & \gamma c_1 \\ \beta e_1 & d_1 + \delta f_1 \end{bmatrix} .$$

Proof. Since node 1 is excitatory the tail of any type A^E arrow is node 1, and since node 2 is inhibitory the tail of any type A^I arrow is node 2. Thus the adjacency matrices are

$$(3.7) \quad \text{Node-type } N^E: A_1 = \begin{bmatrix} 1 & 0 \\ 0 & 0 \end{bmatrix}; \quad \text{Node-type } N^I: A_2 = \begin{bmatrix} 0 & 0 \\ 0 & 1 \end{bmatrix};$$

$$\text{Arrow-type } A^E: A_3 = \begin{bmatrix} \alpha & 0 \\ \beta & 0 \end{bmatrix}; \quad \text{Arrow-type } A^I: A_4 = \begin{bmatrix} 0 & \gamma \\ 0 & \delta \end{bmatrix};$$

where at least β or γ is nonzero to obtain a connected network. These conditions correspond to the network in Figure 4 (left).

Concerning the linearization of equations (3.4) at (x_1, x_2) and the notation in (3.5), symmetry of f and g implies that

$$b_1 = \frac{\partial f}{\partial x_2} \Big|_p = \frac{\partial f}{\partial x_3} \Big|_p = \dots = \frac{\partial f}{\partial x_{\alpha+1}} \Big|_p, \quad c_1 = \frac{\partial f}{\partial x_{\alpha+2}} \Big|_p = \frac{\partial f}{\partial x_{\alpha+3}} \Big|_p = \dots = \frac{\partial f}{\partial x_{\alpha+\gamma+1}} \Big|_p,$$

$$e_1 = \frac{\partial g}{\partial x_2} \Big|_q = \frac{\partial g}{\partial x_3} \Big|_q = \dots = \frac{\partial g}{\partial x_{\beta+1}} \Big|_q, \quad f_1 = \frac{\partial g}{\partial x_{\beta+2}} \Big|_q = \frac{\partial g}{\partial x_{\beta+3}} \Big|_q = \dots = \frac{\partial g}{\partial x_{\beta+\delta+1}} \Big|_q .$$

From this we obtain (3.6). \square

Remark 3.2. The 2-node REI network in Figure 4 (left) for $\alpha = \beta = \gamma = \delta = 1$ is the Smolen network in Figure 2. \diamond

3.2. Connected 2-node REI Networks: ODE-classes. We now deduce the classification of connected 2-node REI networks up to ODE-equivalence.

Proposition 3.3. *There are exactly two ODE-classes of connected 2-node REI networks, with representatives NH1 and NH2 pictured in Figure 5. The associated admissible ODEs are stated in Table 2.*



FIGURE 5. The two ODE-classes of connected 2-node REI networks. Table 2 states the corresponding admissible ODEs. The network NH2 is the minimal network ODE-equivalent to the Smolen network of Figure 2.

NH1	$\dot{x}_1 = f(x_1^+)$ $\dot{x}_2 = g(x_2^-; x_1^+)$	NH2	$\dot{x}_1 = f(x_1^+; x_2^-)$ $\dot{x}_2 = g(x_2^-; x_1^+)$
-----	---	-----	--

TABLE 2. Admissible ODEs for the networks in Figure 5.

Proof. We recall that our classifications are stated up to duality and numbering of the nodes. Any connected 2-node REI network is of the form presented in Figure 4 (left), where $\alpha, \beta, \gamma, \delta$ are nonnegative integers representing arrow multiplicities. The adjacency matrices are stated in (3.7), where at least β or γ is nonzero to guarantee connectedness. Trivially,

$$\langle A_1, A_2, A_3, A_4 \rangle = \left\langle A_1, A_2, \begin{bmatrix} 0 & 0 \\ \beta & 0 \end{bmatrix}, \begin{bmatrix} 0 & \gamma \\ 0 & 0 \end{bmatrix} \right\rangle,$$

where angle brackets denote the real subspace spanned by their contents. Therefore the network in Figure 4 (left) is ODE-equivalent to the network in Figure 4 (right). If $\gamma = 0$, so $\beta \neq 0$, then

$$\langle A_1, A_2, A_3, A_4 \rangle = \left\langle \langle A_1, A_2, \begin{bmatrix} 0 & 0 \\ 1 & 0 \end{bmatrix} \rangle \right\rangle$$

giving network NH1 in Figure 5. (The case $\beta = 0$ and $\gamma \neq 0$ is dual.) If both β and γ are nonzero then

$$\langle A_1, A_2, A_3, A_4 \rangle = \left\langle A_1, A_2, \begin{bmatrix} 0 & 0 \\ 1 & 0 \end{bmatrix}, \begin{bmatrix} 0 & 1 \\ 0 & 0 \end{bmatrix} \right\rangle$$

giving network NH2 in Figure 5. □

3.3. Connected 2-node REI Networks with valence up to 2. Recall that the valence of a node is the number of input arrows to that node. Using the classification in the previous section, we now list all connected 2-node EI networks where all nodes have valence ≤ 2 . In what follows, a bound on the valence such as ≤ 2 means that the valence of *each* node satisfies that bound.

Proposition 3.4. *There are 15 connected 2-node REI networks with valence ≤ 2 . Of these, 9 are in the ODE-class of NH1 in Figure 5, and 6 are in the ODE-class of NH2 in Figure 5. See Figure 6 and Table 3.*

Proof. By Proposition 3.3 a connected 2-node REI network with valence ≤ 2 is ODE-equivalent either to NH1 or to NH2. Each of NH1 and NH2 is a minimal representative of its ODE-class. Network NH1 has only one arrow, which is excitatory and sent by excitatory node 1 to node 2. In an ODE-equivalent network, node 1 can send two excitatory arrows to node 2. Also, up to ODE-equivalence, node 1 can have no autoregulation or one or two autoregulation excitatory arrows, and node 2 can have no autoregulation or one autoregulation inhibitory arrow. Considering all the combinations, with valence up to 2, we find 9 networks that are ODE-equivalent to NH1, namely networks (a)-(i) in Figure 6. NH2 has one excitatory arrow, which is sent by the excitatory node 1 to node 2, and one inhibitory arrow, which is sent by the inhibitory node 2 to node 1. Up to ODE-equivalence, node 1 can receive one more inhibitory arrow from node 2 or one autoregulation excitatory arrow. Also, up to ODE-equivalence, node 2 can receive one more excitatory arrow from node 1 or one autoregulation inhibitory arrow. Considering all the combinations, up to duality, we find 6 networks that are ODE-equivalent to NH2, namely networks (j)-(o) in Figure 6. Table 3 lists their admissible ODEs. \square

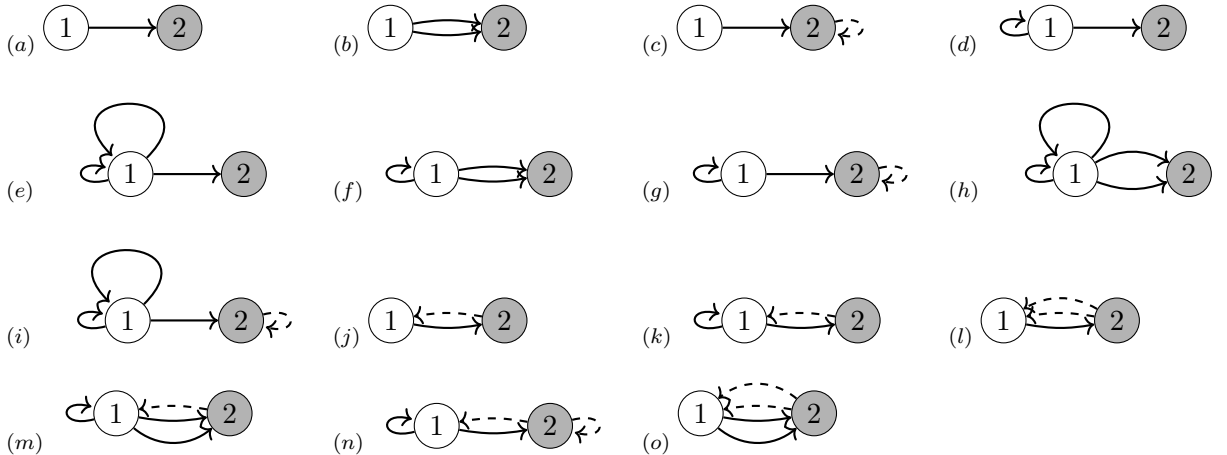


FIGURE 6. Connected 2-node REI networks with input valence ≤ 2 . Networks (a)-(i) are in the ODE-class of network NH1 in Figure 5 and networks (j)-(o) are in the ODE-class of network NH2 in Figure 5.

Remarks 3.5. (i) The networks of the ODE-class of NH1 are feedforward; the networks of the ODE-class of NH2 are transitive.

(a) $\dot{x}_1 = f(x_1^+)$ $\dot{x}_2 = g(x_2^-; x_1^+)$	(b) $\dot{x}_1 = f(x_1^+)$ $\dot{x}_2 = g(x_2^-; x_1^+, x_1^+)$	(c) $\dot{x}_1 = f(x_1^+)$ $\dot{x}_2 = g(x_2^-; x_1^+, x_2^-)$
(d) $\dot{x}_1 = f(x_1^+; x_1^+)$ $\dot{x}_2 = g(x_2^-; x_1^+)$	(e) $\dot{x}_1 = f(x_1^+; \overline{x_1^+, x_1^+})$ $\dot{x}_2 = g(x_2^-; x_1^+)$	(f) $\dot{x}_1 = f(x_1^+; \overline{x_1^+, x_1^+})$ $\dot{x}_2 = g(x_2^-; x_1^+, x_1^+)$
(g) $\dot{x}_1 = f(x_1^+; x_1^+)$ $\dot{x}_2 = g(x_2^-; x_1^+, x_2^-)$	(h) $\dot{x}_1 = f(x_1^+; \overline{x_1^+, x_1^+})$ $\dot{x}_2 = g(x_2^-; x_1^+, x_1^+)$	(i) $\dot{x}_1 = f(x_1^+; \overline{x_1^+, x_1^+})$ $\dot{x}_2 = g(x_2^-; x_1^+, x_2^-)$
(j) $\dot{x}_1 = f(x_1^+; x_2^-)$ $\dot{x}_2 = g(x_2^-; x_1^+)$	(k) $\dot{x}_1 = f(x_1^+; x_1^+, x_2^-)$ $\dot{x}_2 = g(x_2^-; x_1^+)$	(l) $\dot{x}_1 = f(x_1^+; \overline{x_2^-, x_2^-})$ $\dot{x}_2 = g(x_2^-; x_1^+)$
(m) $\dot{x}_1 = f(x_1^+; \overline{x_1^+, x_2^-})$ $\dot{x}_2 = g(x_2^-; x_1^+, x_1^+)$	(n) $\dot{x}_1 = f(x_1^+; x_1^+, x_2^-)$ $\dot{x}_2 = g(x_2^-; x_1^+, x_2^-)$	(o) $\dot{x}_1 = f(x_1^+; \overline{x_2^-, x_2^-})$ $\dot{x}_2 = g(x_2^-; x_1^+, x_1^+)$

TABLE 3. Admissible ODEs for the networks in Figure 6. Since all networks are inhomogeneous, the admissible ODEs are determined by two functions f and g .

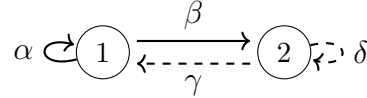


FIGURE 7. A 2-node PEI network. The nonnegative integer arrow multiplicities are $\alpha, \beta, \gamma, \delta$. The network is connected when one of β or γ is nonzero.

(ii) The Smolen network, which is network (n) of Figure 6, belongs to the ODE-class of NH2. There are no \mathbb{Z}_2 -symmetric networks in this classification.

(iii) For any choice of node state spaces, the space of admissible maps for the network of NH1 is strictly contained in the space of admissible maps for the network NH2. \diamond

3.4. Connected 2-node PEI Networks. A 2-node PEI network is the network on the left of Figure 4, considering the two nodes to be of the same type, for a suitable choice of nonnegative integer arrow multiplicities $\alpha, \beta, \gamma, \delta$. See Figure 7.

There is an analogous result to Proposition 3.1 for REI networks, with the same proof.

Proposition 3.6. *A 2-node connected PEI network is the network of Figure 7, for some choice of nonnegative integer arrow multiplicities $\alpha, \beta, \gamma, \delta$, where one of β or γ is nonzero. All the statements of Proposition 3.1 hold, with the additional condition that the two nodes have the same node-type. When the multiplicities satisfy $\alpha = \beta$, $\gamma = \delta$ then the network is homogeneous and (3.4) holds with $f = g$.*

3.5. Connected 2-node PEI Networks: ODE-classes. The classification of PEI networks into ODE-classes is different from that of REI networks since a 2-node PEI network, see Figure 7, has three network adjacency matrices:

$$(3.8) \quad \begin{aligned} \text{Node-type } N^E = N^I: \text{Id}_2 &= \begin{bmatrix} 1 & 0 \\ 0 & 1 \end{bmatrix}; \\ \text{Arrow-type } A^E: A_3 &= \begin{bmatrix} \alpha & 0 \\ \beta & 0 \end{bmatrix}; \quad \text{Arrow-type } A^I: A_4 = \begin{bmatrix} 0 & \gamma \\ 0 & \delta \end{bmatrix}; \end{aligned}$$

where at least β or γ is nonzero to obtain a connected network. Therefore there are infinitely many distinct ODE-classes for 2-node PEI networks:

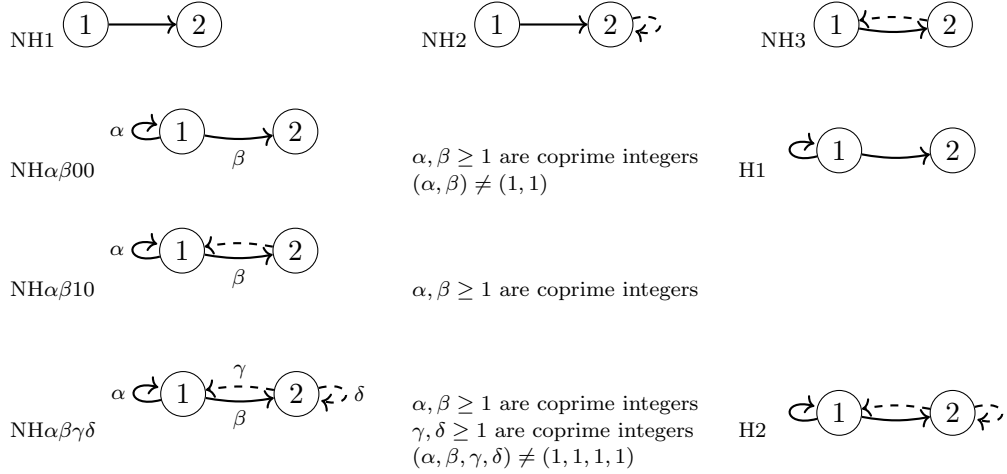


FIGURE 8. Network representatives, of the ODE-classes of connected 2-node PEI networks, up to duality.

Proposition 3.7. *There is an infinity of ODE-classes of connected 2-node PEI networks, with representatives in Figure 8 and associated admissible ODEs in Table 4.*

Proof. Given an ODE-class of 2-node PEI networks, consider a network in that class and the corresponding adjacency matrices Id_2, A_3 and A_4 as in (3.8). Since the network is connected, we have that at least one of β, γ is nonzero. The proof divides

NH1	$\dot{x}_1 = f(x_1)$ $\dot{x}_2 = g(x_2; x_1^+)$	NH2	$\dot{x}_1 = f(x_1)$ $\dot{x}_2 = g(x_2; x_1^+, x_2^-)$
NH3	$\dot{x}_1 = f(x_1; x_2^-)$ $\dot{x}_2 = g(x_2; x_1^+)$	NH $\alpha\beta$ 00	$\dot{x}_1 = f(x_1; \underbrace{x_1^+, \dots, x_1^+}_{\alpha})$ $\dot{x}_2 = g(x_2; \underbrace{x_1^+, \dots, x_1^+}_{\beta})$
NH $\alpha\beta$ 10	$\dot{x}_1 = f(x_1; \underbrace{x_1^+, \dots, x_1^+}_{\alpha}, x_2^-)$ $\dot{x}_2 = g(x_2; \underbrace{x_1^+, \dots, x_1^+}_{\beta})$	NH $\alpha\beta\gamma\delta$	$\dot{x}_1 = f(x_1; \underbrace{x_1^+, \dots, x_1^+}_{\alpha}; \underbrace{x_2^-, \dots, x_2^-}_{\gamma})$ $\dot{x}_2 = g(x_2; \underbrace{x_1^+, \dots, x_1^+}_{\beta}; \underbrace{x_2^-, \dots, x_2^-}_{\delta})$
H1	$\dot{x}_1 = f(x_1; x_1^+);$ $\dot{x}_2 = f(x_2; x_1^+)$	H2	$\dot{x}_1 = f(x_1; x_1^+, x_2^-);$ $\dot{x}_2 = f(x_2; x_1^+, x_2^-)$

TABLE 4. Admissible ODEs for the networks in Figure 8.

into four cases according to how many of the integers $\alpha, \beta, \gamma, \delta$ are zero.

(i) If all four integers are positive, then the matrices Id_2, A_3 and A_4 are linearly independent. Moreover, the matrices of the minimal network of that ODE-class are those obtained from A_3 , multiplied by $1/\text{gcd}(\alpha, \beta)$, and A_4 , multiplied by $1/\text{gcd}(\gamma, \delta)$. We obtain the ODE-classes of inhomogeneous networks NH $\alpha\beta\gamma\delta$ in Figure 8, which are parametrized by the positive integers $\alpha, \beta, \gamma, \delta$, where α, β are coprime, γ, δ are coprime, and $(\alpha, \beta, \gamma, \delta) \neq (1, 1, 1, 1)$. If $(\alpha, \beta, \gamma, \delta) = (1, 1, 1, 1)$ then we obtain the homogeneous network ODE-class H2 of Figure 8.

(ii) If exactly one of the integers $\alpha, \beta, \gamma, \delta$ is zero, then, up to duality, either $\gamma = 0$ or $\delta = 0$. In the first case,

$$\left\langle \text{Id}_2, \begin{bmatrix} \alpha & 0 \\ \beta & 0 \end{bmatrix}, \begin{bmatrix} 0 & 0 \\ 0 & \delta \end{bmatrix} \right\rangle = \left\langle \text{Id}_2, \begin{bmatrix} 0 & 0 \\ 1 & 0 \end{bmatrix}, \begin{bmatrix} 0 & 0 \\ 0 & 1 \end{bmatrix} \right\rangle$$

and every such network is ODE-equivalent to network NH2 in Figure 8. In the second case,

$$\left\langle \text{Id}_2, \begin{bmatrix} \alpha & 0 \\ \beta & 0 \end{bmatrix}, \begin{bmatrix} 0 & \gamma \\ 0 & 0 \end{bmatrix} \right\rangle = \left\langle \text{Id}_2, \begin{bmatrix} \alpha & 0 \\ \beta & 0 \end{bmatrix}, \begin{bmatrix} 0 & 1 \\ 0 & 0 \end{bmatrix} \right\rangle.$$

Now we obtain the ODE-classes NH $\alpha\beta$ 10 in Figure 8, which are parametrized by the positive integers α, β , where α, β are coprime.

(iii) Suppose that exactly two of the integers $\alpha, \beta, \gamma, \delta$ are zero. Up to duality, either

$\gamma = \delta = 0$, or $\gamma = \alpha = 0$, or $\delta = \alpha = 0$. If $\gamma = \delta = 0$ and $(\alpha, \beta) \neq (1, 1)$ we obtain the ODE-classes $\text{NH}\alpha\beta 00$ in Figure 8, which are parametrized by the positive integers α, β where α, β are coprime. If $\gamma = \delta = 0$ and $(\alpha, \beta) = (1, 1)$, we obtain the ODE-class containing the homogeneous network H1 in Figure 8. If $\gamma = \alpha = 0$, then since

$$\left\langle \text{Id}_2, \begin{bmatrix} 0 & 0 \\ \beta & 0 \end{bmatrix}, \begin{bmatrix} 0 & 0 \\ 0 & \delta \end{bmatrix} \right\rangle = \left\langle \text{Id}_2, \begin{bmatrix} 0 & 0 \\ 1 & 0 \end{bmatrix}, \begin{bmatrix} 0 & 0 \\ 0 & 1 \end{bmatrix} \right\rangle,$$

we have networks in the ODE-class of network NH2 in Figure 8.

Similarly, if $\delta = \alpha = 0$, then since

$$\left\langle \text{Id}_2, \begin{bmatrix} 0 & 0 \\ \beta & 0 \end{bmatrix}, \begin{bmatrix} 0 & \gamma \\ 0 & 0 \end{bmatrix} \right\rangle = \left\langle \text{Id}_2, \begin{bmatrix} 0 & 0 \\ 1 & 0 \end{bmatrix}, \begin{bmatrix} 0 & 1 \\ 0 & 0 \end{bmatrix} \right\rangle,$$

we have networks at the ODE-class of network NH3 in Figure 8.

(iv) Suppose that exactly three of the integers $\alpha, \beta, \gamma, \delta$ are zero. Up to duality, we can consider only the cases where $\delta = \gamma = 0$ and $\alpha = 0$, since the networks are connected. Now

$$\left\langle \text{Id}_2, \begin{bmatrix} 0 & 0 \\ \beta & 0 \end{bmatrix} \right\rangle = \left\langle \text{Id}_2, \begin{bmatrix} 0 & 0 \\ 1 & 0 \end{bmatrix} \right\rangle,$$

so we have networks in the ODE-class of network NH1 in Figure 8. \square

3.6. Connected 2-node PEI Networks with valence up to 2.

Proposition 3.8. *The set of 2-node connected PEI networks with node input valence up to 2 contains 15 networks, which correspond to the networks in Figure 6 but assuming the nodes to be of the same type. This set is partitioned into 9 ODE-classes: 7 classes formed by inhomogeneous networks and 2 by homogeneous networks, see Figure 9 and Table 5.*

Proof. Trivially, the 2-node connected PEI networks with node input valence up to 2 can be obtained from the 2-node connected REI networks with node input valence up to 2 (see Figure 6) by considering the nodes to have the same type. The main result of Dias and Stewart [13] on ODE-equivalence implies that there are 9 ODE-classes of PEI networks: a class containing networks (a) and (b), a class containing networks (d) and (h), a class containing networks (j), (l) and (o), a class containing networks (c), (g) and (i). Each of the remaining five networks represents a different ODE-class. See Figure 9 for minimal ODE-class representatives. Table 5 lists the admissible maps for the networks in Figure 9. \square

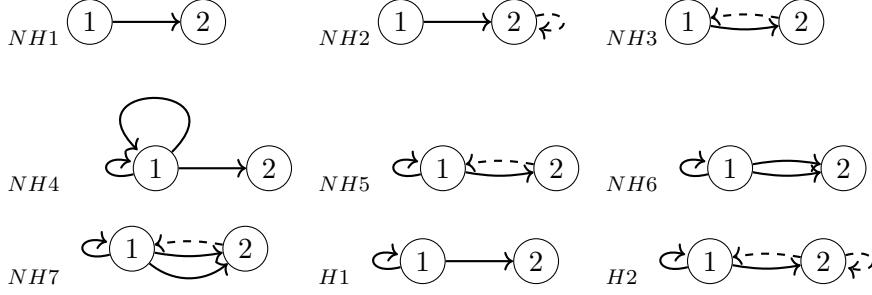


FIGURE 9. There are 9 ODE-classes of 2-node connected PEI networks with input valence up to two: 7 inhomogeneous classes and 2 homogeneous classes. Table 5 lists the corresponding admissible maps.

NH1	$\dot{x}_1 = f(x_1);$ $\dot{x}_2 = g(x_2; x_1^+)$	NH2	$\dot{x}_1 = f(x_1);$ $\dot{x}_2 = g(x_2; x_1^+, x_2^-)$	NH3	$\dot{x}_1 = f(x_1; x_2^-);$ $\dot{x}_2 = g(x_2; x_1^+)$
NH4	$\dot{x}_1 = f(x_1; x_1^+, x_1^+);$ $\dot{x}_2 = g(x_2; x_1^+)$	NH5	$\dot{x}_1 = f(x_1; x_1^+, x_2^-);$ $\dot{x}_2 = g(x_2; x_1^+)$	NH6	$\dot{x}_1 = f(x_1; x_1^+);$ $\dot{x}_2 = g(x_2; x_1^+, x_1^+)$
NH7	$\dot{x}_1 = f(x_1; x_1^+, x_2^-);$ $\dot{x}_2 = g(x_2; x_1^+, x_1^+)$	H1	$\dot{x}_1 = f(x_1; x_1^+);$ $\dot{x}_2 = f(x_2; x_1^+)$	H2	$\dot{x}_1 = f(x_1; x_1^+, x_2^-);$ $\dot{x}_2 = f(x_2; x_1^+, x_2^-)$

TABLE 5. Admissible maps for the networks in Figure 9.

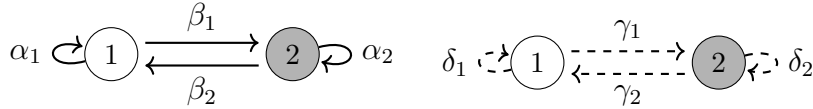


FIGURE 10. A 2-node UEI network has two 2-node subnetworks.

3.7. Connected 2-node UEI Networks. We now consider 2-node UEI networks. Here, node 1 is excitatory and node 2 is inhibitory. To classify these we split the network into two subnetworks, each containing both nodes. One subnetwork retains only the excitatory arrows, the other retains only the inhibitory ones. We classify each subnetwork separately and reassemble them.

Proposition 3.9. *A connected 2-node UEI network splits into the two subnetworks in Figure 10, for suitable nonnegative integer arrow multiplicities $\alpha_i, \beta_i, \gamma_i, \delta_i$, where*

$i = 1, 2$ and at least one of the $\beta_1, \beta_2, \gamma_1, \gamma_2$ is nonzero. The admissible ODEs are:

$$(3.9) \quad \begin{aligned} \dot{x}_1 &= f(x_1^+; \underbrace{x_1^+, \dots, x_1^+}_{\alpha_1}, \underbrace{x_2^+, \dots, x_2^+}_{\beta_2}, \underbrace{x_1^-, \dots, x_1^-}_{\delta_1}, \underbrace{x_2^-, \dots, x_2^-}_{\gamma_2}) \\ \dot{x}_2 &= g(x_2^-; \underbrace{x_1^+, \dots, x_1^+}_{\beta_1}, \underbrace{x_2^+, \dots, x_2^+}_{\alpha_2}, \underbrace{x_1^-, \dots, x_1^-}_{\gamma_1}, \underbrace{x_2^-, \dots, x_2^-}_{\delta_2}) \end{aligned}$$

Here $x_1^+, x_2^- \in \mathbb{R}^k$, so the total state space is \mathbb{R}^{2k} , and f and g are smooth functions invariant under permutation of the variables under each overline.

To simplify notation, temporarily omit the \pm superscripts, and define

$$(3.10) \quad \begin{aligned} p &= (x_1, \underbrace{x_1, \dots, x_1}_{\alpha_1}, \underbrace{x_2, \dots, x_2}_{\beta_2}, \underbrace{x_1, \dots, x_1}_{\delta_1}, \underbrace{x_2, \dots, x_2}_{\gamma_2}) \\ q &= (x_2, \underbrace{x_1, \dots, x_1}_{\beta_1}, \underbrace{x_2, \dots, x_2}_{\alpha_2}, \underbrace{x_1, \dots, x_1}_{\gamma_1}, \underbrace{x_2, \dots, x_2}_{\delta_2}) \\ a &= \frac{\partial f}{\partial x_1} \Big|_p & b_1 &= \frac{\partial f}{\partial x_2} \Big|_p & b_2 &= \frac{\partial f}{\partial x_{2+\alpha_1}} \Big|_p \\ c_1 &= \frac{\partial f}{\partial x_{2+\alpha_1+\beta_2}} \Big|_p & c_2 &= \frac{\partial f}{\partial x_{2+\alpha_1+\beta_2+\delta_1}} \Big|_p \\ d &= \frac{\partial g}{\partial x_1} \Big|_q & e_1 &= \frac{\partial g}{\partial x_2} \Big|_q & e_2 &= \frac{\partial g}{\partial x_{2+\beta_1}} \Big|_q \\ f_1 &= \frac{\partial g}{\partial x_{2+\beta_1+\alpha_2}} \Big|_q & f_2 &= \frac{\partial g}{\partial x_{2+\beta_1+\alpha_2+\gamma_1}} \Big|_q \end{aligned}$$

the linearization of (3.4) at (x_1, x_2) is the $2k \times 2k$ matrix

$$(3.11) \quad \begin{bmatrix} a + \alpha_1 b_1 + \delta_1 c_1 & \beta_2 b_2 + \gamma_2 c_2 \\ \beta_1 e_1 + \gamma_1 f_1 & d + \alpha_2 e_2 + \delta_2 f_2 \end{bmatrix}.$$

Proof. For a UEI network there is no restriction on the tail node-type for A^E arrows and A^I arrows. The adjacency matrices are therefore

$$(3.12) \quad \begin{aligned} \text{Node-type } N^E: A_1 &= \begin{bmatrix} 1 & 0 \\ 0 & 0 \end{bmatrix}; & \text{Node-type } N^I: A_2 &= \begin{bmatrix} 0 & 0 \\ 0 & 1 \end{bmatrix}; \\ \text{Arrow-type } A^E: A_3 &= \begin{bmatrix} \alpha_1 & \beta_2 \\ \beta_1 & \alpha_2 \end{bmatrix}; & \text{Arrow-type } A^I: A_4 &= \begin{bmatrix} \delta_1 & \gamma_2 \\ \gamma_1 & \delta_2 \end{bmatrix}; \end{aligned}$$

where at least one of the β_i or γ_i is nonzero to guarantee connectedness. The network is the union of two 2-node subnetworks, one containing the arrows of type A^E and the other of type A^I , which correspond to the networks in Figure 10.

Concerning the linearization of equations (3.9) at (x_1, x_2) , the symmetries of the functions f and g imply (3.11). \square

3.8. Connected 2-node UEI Networks: ODE-classes.

Proposition 3.10. *There is an infinity of ODE-classes of connected 2-node UEI networks, with representatives in Figure 11 and associated admissible ODEs in Table 6.*

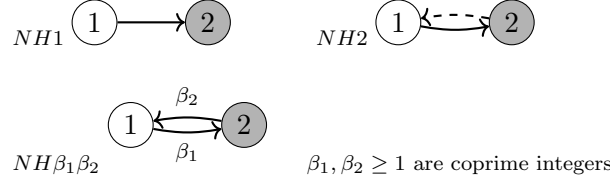


FIGURE 11. Network representatives, of the ODE-classes of connected 2-node UEI networks, up to duality. The representatives NH1 and NH2 are REI networks.

NH1	$\dot{x}_1 = f(x_1^+)$ $\dot{x}_2 = g(x_2^-; x_1^+)$	NH2	$\dot{x}_1 = f(x_1^+; x_2^-)$ $\dot{x}_2 = g(x_2^-; x_1^+)$
NH $\beta_1\beta_2$	$\dot{x}_1 = f(x_1^+; \underbrace{x_2^+, \dots, x_2^+}_{\beta_2})$ $\dot{x}_2 = g(x_2^-; \underbrace{x_1^+, \dots, x_1^+}_{\beta_1})$		

TABLE 6. Admissible ODEs for the networks in Figure 11.

Proof. Clearly

$$\langle A_1, A_2, A_3, A_4 \rangle = \left\langle A_1, A_2, \begin{bmatrix} 0 & \beta_2 \\ \beta_1 & 0 \end{bmatrix}, \begin{bmatrix} 0 & \gamma_2 \\ \gamma_1 & 0 \end{bmatrix} \right\rangle,$$

where the A_i are given by (3.12).

(i) If $\beta_2 = 0$ and $\beta_1 \neq 0$ (duality deals with the case $\beta_2 \neq 0$ and $\beta_1 = 0$) then

$$\langle A_1, A_2, A_3, A_4 \rangle = \left\langle A_1, A_2, \begin{bmatrix} 0 & 0 \\ 1 & 0 \end{bmatrix}, \begin{bmatrix} 0 & \gamma_2 \\ 0 & 0 \end{bmatrix} \right\rangle.$$

(i.a) If $\gamma_2 = 0$ then

$$\langle A_1, A_2, A_3, A_4 \rangle = \left\langle A_1, A_2, \begin{bmatrix} 0 & 0 \\ 1 & 0 \end{bmatrix} \right\rangle,$$

which corresponds to network NH1 in Figure 11.

(i.b) If $\gamma_2 \neq 0$ we get network NH2 in Figure 11 with adjacency matrices

$$A_1, A_2, \begin{bmatrix} 0 & 0 \\ 1 & 0 \end{bmatrix}, \begin{bmatrix} 0 & 1 \\ 0 & 0 \end{bmatrix}.$$

The linear space

$$\left\langle A_1, A_2, \begin{bmatrix} 0 & 0 \\ 1 & 0 \end{bmatrix}, \begin{bmatrix} 0 & 1 \\ 0 & 0 \end{bmatrix} \right\rangle$$

is 4-dimensional; that is, it coincides with the linear space of all 2×2 -matrices with real entries.

(ii) If both β_1, β_2 are nonzero, we distinguish two cases:

(ii.a) When $\gamma_1 = \gamma_2 = 0$ we obtain networks with adjacency matrices

$$A_1, A_2, \begin{bmatrix} 0 & \beta_2 \\ \beta_1 & 0 \end{bmatrix}.$$

In particular, we obtain the networks NH3 (if $\beta_1 = \beta_2 = 1$) and NH4 (if $\beta_1 = 2, \beta_2 = 1$) pictured in Figure 12. There is an infinite number of ODE-equivalence classes, with representatives the networks for each arrow-type adjacency matrix

$$\begin{bmatrix} 0 & \beta_2 \\ \beta_1 & 0 \end{bmatrix}$$

where $\beta_1, \beta_2 \geq 1$ are coprime, yielding the network $\text{NH}\beta_1\beta_2$.

(ii.b) If at least one of the γ_1 or γ_2 is nonzero, either $\langle A_1, A_2, A_3, A_4 \rangle = \langle A_1, A_2, A_3 \rangle$, leading to one of the previous cases, or $\dim \langle A_1, A_2, A_3, A_4 \rangle = 4$, and we have a network ODE-equivalent to NH2. This was obtained previously, since

$$\langle A_1, A_2, A_3, A_4 \rangle = \left\langle A_1, A_2, \begin{bmatrix} 0 & 0 \\ 1 & 0 \end{bmatrix}, \begin{bmatrix} 0 & 1 \\ 0 & 0 \end{bmatrix} \right\rangle.$$

(iii) In the final case when $\beta_1 = \beta_2 = 0$ we obtain the dual cases of the networks in (ii.a). \square

3.9. Connected 2-node UEI Networks with valence up to 2. Using the results in the previous section, we list all the connected 2-node UEI networks with valence ≤ 2 .

Proposition 3.10 implies:

Proposition 3.11. *There are 4 ODE-classes of connected 2-node UEI networks with valence ≤ 2 . Representatives are in Figure 12, and associated admissible ODEs are listed in Table 7.*

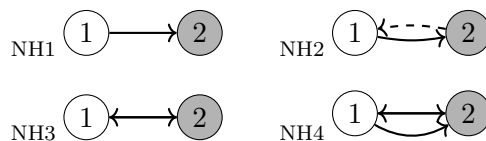


FIGURE 12. Minimal network representatives of the 4 ODE-classes of connected 2-node UEI networks with input valence ≤ 2 . The representatives NH1 and NH2 are REI networks.

Proof. Consider the ODE-classes of the connected 2-node UEI networks given by Proposition 3.10, with representatives in Figure 11. These representatives are minimal, in the sense of having a minimum number of arrows. Thus it is enough to check which of these ODE-classes has a minimal representative with valence ≤ 2 .

Clearly NH1 and NH2 in Figure 11 are representatives of two of the ODE-classes of connected 2-node UEI networks with valence ≤ 2 .

There are only two ODE-class representatives obtained from $\text{NH}\beta_1\beta_2$ in Figure 11, one with $\beta_1 = \beta_2 = 1$ and the other with $\beta_1 = 2, \beta_2 = 1$. These are networks NH3 and NH4 in Figure 12. \square

NH1	$\dot{x}_1 = f(x_1^+)$ $\dot{x}_2 = g(x_2^-; x_1^+)$	NH2	$\dot{x}_1 = f(x_1^+; x_2^-)$ $\dot{x}_2 = g(x_2^-; x_1^+)$
NH3	$\dot{x}_1 = f(x_1^+; x_2^+)$ $\dot{x}_2 = g(x_2^-; x_1^+)$	NH4	$\dot{x}_1 = f(x_1^+; x_2^+)$ $\dot{x}_2 = g(x_2^-; x_1^+, x_1^+)$

TABLE 7. Admissible ODEs for the networks in Figure 12.

Proposition 3.12. *There are 53 connected 2-node UEI networks with valence ≤ 2 : the 15 REI networks in Figure 6, given by Proposition 3.4, and the 38 networks in Figure 13. Considering the 4 ODE-classes in Figure 12, the ODE-class NH1 contains 9 of the UEI networks in Figure 6 and the ODE-class NH2 contains the other 6. The partition of 38 UEI networks in Figure 13 into 4 ODE-classes is stated in Table 8.*

Proof. By Definition 2.3, REI networks are UEI networks. Thus, we start by considering the 15 connected 2-node UEI networks with valence ≤ 2 in Figure 6, given by Proposition 3.4. Next, from those 15 networks we get the remaining UEI networks with valence ≤ 2 , up to renumbering of nodes and duality. We maintain the assumption that node 1 is excitatory and node 2 is inhibitory, but since we work with UEI networks we remove the node-type restriction on outputs. The result is Figure 13.

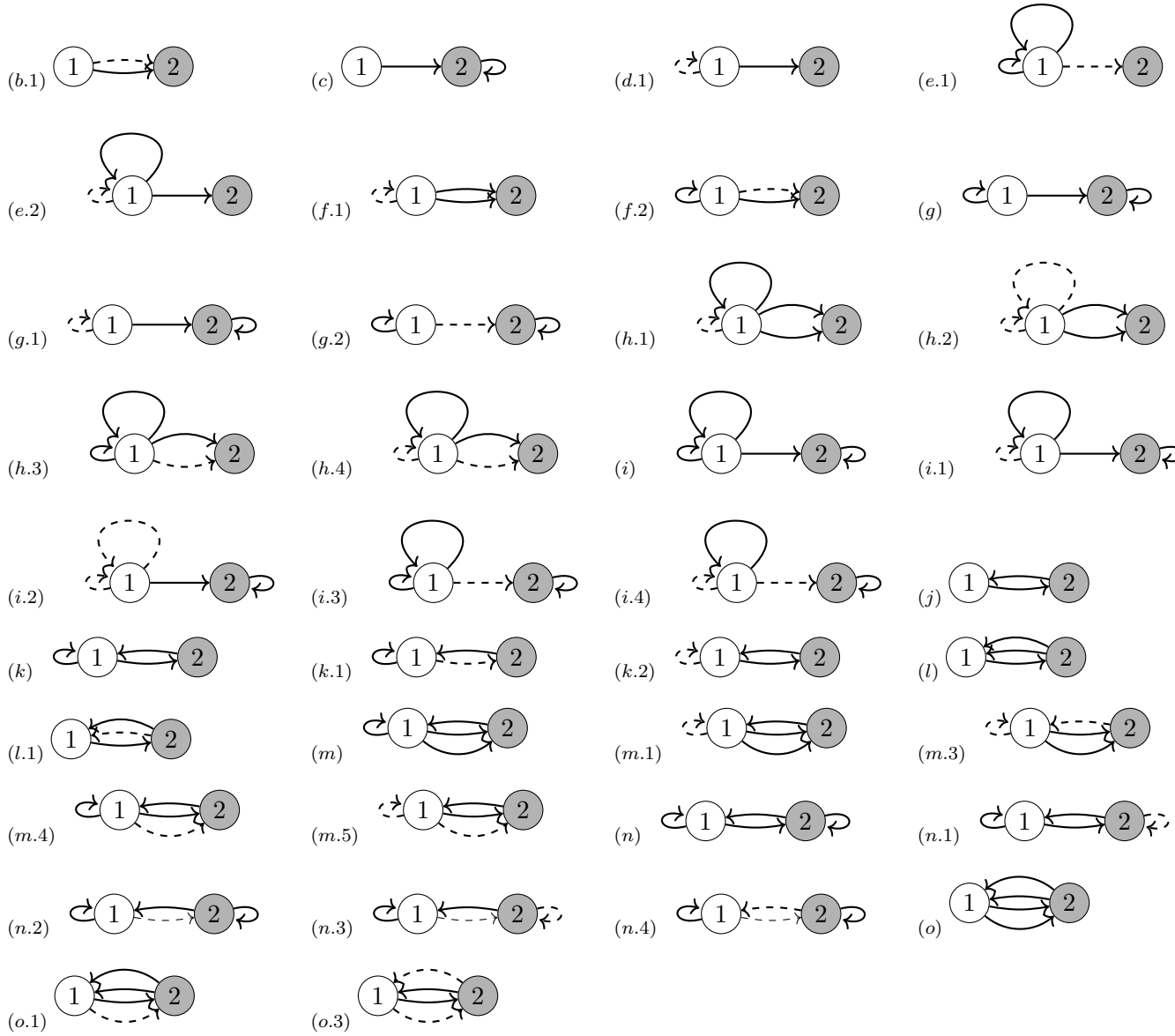


FIGURE 13. 38 connected 2-node UEI networks with input valence ≤ 2 . This set is partitioned into 4 ODE-classes as in Table 8. Representatives of the ODE-classes are in Figure 12.

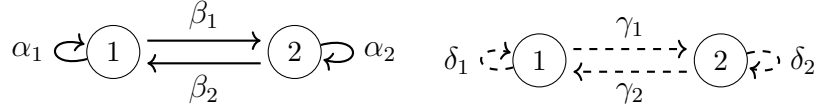


FIGURE 14. A 2-node CEI network has two 2-node subnetworks.

Representatives of the minimal ODE-classes of the 53 networks are in Figure 12. By Proposition 3.4, the set of 15 networks in Figure 6 is partitioned into the ODE-classes NH1 and NH2. By the results of [13], the set of 38 networks in Figure 13 is partitioned into the 4 ODE-classes according to Table 8. Table 7 states the corresponding admissible ODEs. \square

NH1	$(b.1) - (i.4)$	NH2	$(k.1), (l.1), (m.3) - (m.5),$ $(n.2) - (n.3), (o.1)$
NH3	$(j) - (k), (k.2),$ $(n) - (n.1), (n.4), (o), (o.3)$	NH4	$(l), (m) - (m.1)$

TABLE 8. Partition of the connected 2-node UEI networks with valence ≤ 2 , listed in Figure 13, into the four network ODE-classes in Figure 12.

Corollary 3.13. *Only one ODE class of connected 2-node UEI networks of valence ≤ 2 has a minimal representative with two types of arrow, namely NH2. This is also an REI network.*

Remarks 3.14. (i) There are 2 ODE-classes of connected 2-node UEI networks of valence ≤ 2 which coincide with the 2 ODE-classes of connected 2-node REI networks of valence ≤ 2 .

(ii) There are 2 ODE-classes of connected 2-node UEI networks of valence ≤ 2 which are not REI. Moreover, they have representatives with only one arrow-type. \diamond

3.10. Connected 2-node CEI Networks. A 2-node connected CEI network is the union of two subnetworks as in Figure 10, but considering the two nodes to be of the same type. The arrow multiplicities are nonnegative integers $\alpha_i, \beta_i, \gamma_i, \delta_i$, where $i = 1, 2$ and at least one of the $\beta_1, \beta_2, \gamma_1, \gamma_2$ is nonzero, see Figure 14.

There is an analogous result to Proposition 3.9 for UEI networks with the same proof.

Proposition 3.15. *A 2-node connected CEI network is the network of Figure 14, for some choice of nonnegative integer arrow multiplicities $\alpha_i, \beta_i, \gamma_i, \delta_i$, where $i = 1, 2$*

and at least one of the $\beta_1, \beta_2, \gamma_1, \gamma_2$ is nonzero. All the statements of Proposition 3.9 hold, with the additional condition that the two nodes have the same node-type. When the multiplicities satisfy $\alpha_1 + \beta_2 = \alpha_2 + \beta_1$ and $\delta_1 + \gamma_2 = \gamma_1 + \delta_2$, then the network is homogeneous and (3.9) holds with $f = g$.

3.11. Connected 2-node CEI Networks: ODE-classes. For a 2-node CEI network there is no restriction on the tail node-type for A^E arrows and A^I arrows, and the two nodes have the same type. The adjacency matrices are therefore

$$\text{Node-type } N^E = N^I: \text{Id}_2;$$

$$\text{Arrow-type } A^E: A_3 = \begin{bmatrix} \alpha_1 & \beta_2 \\ \beta_1 & \alpha_2 \end{bmatrix}; \quad \text{Arrow-type } A^I: A_4 = \begin{bmatrix} \delta_1 & \gamma_2 \\ \gamma_1 & \delta_2 \end{bmatrix};$$

where at least one of the β_i or γ_i is nonzero to guarantee connectedness.

Following Definition 4.2 in [2], given a network G and the corresponding ODE-class $[G]$, we denote by $m[G]$ the minimal number of edges for the networks in $[G]$. Following Definition 5.10 in [2], given a matrix $M = [m_{ij}]_{1 \leq i, j \leq n} \in M_{nn}(\mathbb{R})$, let $l(M) = \sum_{i=1}^n \sum_{j=1}^n m_{ij}$. [2, Proposition 5.11] implies:

Proposition 3.16. *There is an infinity of ODE-classes of connected 2-node CEI networks. Moreover, given a 2-node CEI network G with arrow adjacency matrices A_3 and A_4 , let*

$$m = \dim\langle \text{Id}_2, A_3, A_4 \rangle - 1.$$

Then a minimal EI network ODE-equivalent to G has arrow adjacency matrices M_1, M_2 such that:

- (i) $\{\text{Id}_2, M_1, M_2\}$ is a basis of the real vector space $\langle \text{Id}_2, A_3, A_4 \rangle$.
- (ii) $\sum_{k=1}^m l(M_k) = m[G]$.

3.12. Connected 2-node CEI Networks with valence up to 2.

Proposition 3.17. *The set of 2-node connected CEI networks with node input valence up to two contains 53 networks, which correspond to the 15 UEI networks in Figure 6 and the 38 UEI networks in Figure 13, given by Proposition 3.12, but assuming the nodes to be of the same type.*

Moreover, it is partitioned into 21 ODE-classes. The 15 CEI networks in Figure 6 are PEI networks and are partitioned into 9 ODE-classes: 7 classes formed by inhomogeneous networks and 2 by homogeneous networks, see Figure 9. The 38 CEI networks in Figure 13 are partitioned into 15 ODE-classes, 3 of them PEI ODE-classes: 11 classes formed by inhomogeneous networks and 4 by homogeneous networks, see Figure 15. The corresponding admissible maps appear in Table 9.

Proof. Trivially, the 2-node connected CEI networks with node input valence up to 2 can be obtained from the 2-node connected UEI networks with node input valence

up to 2, see Figures 6 and 13, by considering the nodes to have the same type. The 15 CEI networks in Figure 6 are PEI networks. By Proposition 3.8, they are partitioned into 9 ODE-classes: 7 classes formed by inhomogeneous networks and 2 by homogeneous networks, see Figure 9.

By the result in [13] on networks ODE-equivalence, the 38 CEI networks in Figure 13 are partitioned into 15 ODE-classes of CEI networks, where 3 of them are PEI ODE-classes: one class containing the networks $(b.1), (g), (g.2)$, one class with networks $(d.1), (e.2), (f.1), (f.2), (h.1), (h.2), (i.1), (i.3), (e.1), (h.3)$, one class with networks $(g.1), (i.2)$, one class with networks $(h.4), (i), (i.4)$, one class with networks $(j), (n), (n.4), (o), (o.3)$, one class with networks $(k.1), (m.3), (m.4)$, one with networks $(l.1), (n.2), (o.1)$, and one with $(k.2), (n.1)$. Each of the remaining networks, $(c), (k), (l), (m), (m.1), (m.5), (n.3)$, represents a different ODE-class. See Figure 15 for minimal ODE-class representatives and Table 9 for the admissible maps. \square

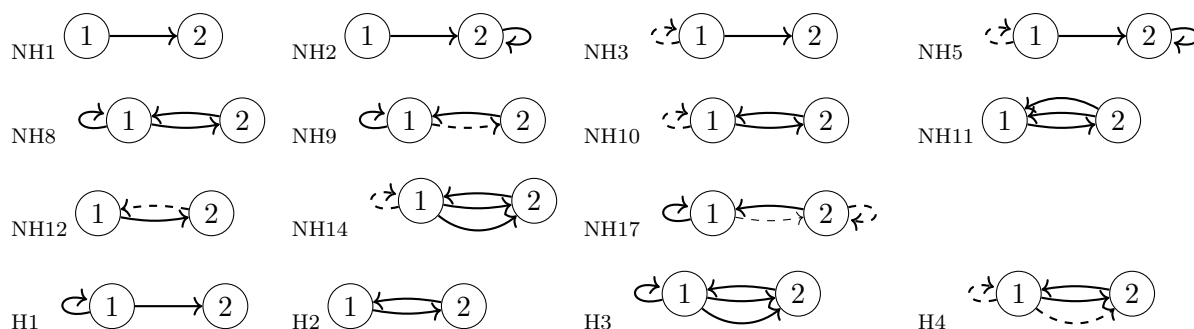


FIGURE 15. Minimal representatives of the 15 ODE-classes of the 38 2-node connected CEI networks with input valence up to two in Figure 13 (assuming the nodes to be of the same type): 11 inhomogeneous and 4 homogeneous. See Table 9 for the corresponding admissible maps. Representatives NH1, H1, and NH12 are PEI networks.

4. CONCLUSIONS

This work is motivated by the importance of biological networks in science. Commonly, in these networks, a distinction is made on the type of connections (excitatory and inhibitory) and on the type of nodes (activator and repressor). We make a general study of 2-node excitatory inhibitory networks (EI) with two types of connections and some more conditions. More precisely, we formalize the structure of EI networks as a preparation of a systematic analysis of dynamics and bifurcations in such networks. Moreover, our results are extended to the 3-node case in [6]. We consider the network formalism where nodes and connections are partitioned into several types

NH1	$\dot{x}_1 = f(x_1)$ $\dot{x}_2 = g(x_2; x_1^+)$	NH2	$\dot{x}_1 = f(x_1)$ $\dot{x}_2 = g(x_2; x_1^+, x_2^+)$	NH3	$\dot{x}_1 = f(x_1; x_1^-)$ $\dot{x}_2 = g(x_2; x_1^+)$
NH5	$\dot{x}_1 = f(x_1; x_1^-)$ $\dot{x}_2 = g(x_2; x_1^+, x_2^+)$	NH8	$\dot{x}_1 = f(x_1; x_1^+, x_2^+)$ $\dot{x}_2 = g(x_2; x_1^+)$	NH9	$\dot{x}_1 = f(x_1; x_1^+, x_2^+)$ $\dot{x}_2 = g(x_2; x_1^-)$
NH10	$\dot{x}_1 = f(x_1; x_1^-, x_2^+)$ $\dot{x}_2 = g(x_2; x_1^+)$	NH11	$\dot{x}_1 = f(x_1; x_2^+, x_2^+)$ $\dot{x}_2 = g(x_2; x_1^+)$	NH12	$\dot{x}_1 = f(x_1; x_2^-)$ $\dot{x}_2 = g(x_2; x_1^+)$
NH14	$\dot{x}_1 = f(x_1; x_1^-, x_2^+)$ $\dot{x}_2 = g(x_2; x_1^+, x_1^+)$	NH17	$\dot{x}_1 = f(x_1; x_1^+, x_2^+)$ $\dot{x}_2 = g(x_2; x_1^-, x_2^-)$	H1	$\dot{x}_1 = f(x_1; x_1^+)$ $\dot{x}_2 = f(x_2; x_1^+)$
H2	$\dot{x}_1 = f(x_1; x_2^+)$ $\dot{x}_2 = f(x_2; x_1^+)$	H3	$\dot{x}_1 = f(x_1; x_1^+, x_2^+)$ $\dot{x}_2 = f(x_2; x_1^+, x_1^+)$	H4	$\dot{x}_1 = f(x_1; x_1^-, x_2^+)$ $\dot{x}_2 = f(x_2; x_1^+, x_1^-)$

TABLE 9. Admissible maps for the networks in Figure 15.

and where the dynamics of the networks respects these and the network topology. In this paper we classify four classes of 2-node EI networks – REI, UEI, PEI, CEI – all with two types of connections (excitatory and inhibitory): for the REI network class, a node cannot output both types of connections whereas for the UEI class a node can output both; moreover, for both REI and UEI networks, there are two node-types (activators and repressors); when all nodes are assumed to be of the same type, then we have the PEI and CEI network classes: if a node cannot output both types of connections the network is PEI, otherwise, the network is CEI. The number of networks of every such network class is not finite. Trivially, restricting the network valence, then each of the four classes has a finite number of networks.

Remarkably, considering the classification up to ODE-equivalence, we obtain that there are only 2 ODE-classes of REI networks while for the other three network classes, there are infinite number of ODE-classes.

Restricting to networks of valency ≤ 2 then the four network classes are formed by finite number of networks. We obtain that the classification of CEI (resp. PEI) networks is derived from the classification of the UEI (resp. REI) networks by assuming the two nodes are of the same type, however, for CEI (resp. PEI) networks there are 21 (resp. 9) ODE-classes and for the UEI (resp. REI) networks there are only 4 (resp. 2) ODE-classes.

Acknowledgments

MA and AD were partially supported by CMUP, member of LASI, which is financed by national funds through FCT – Fundação para a Ciência e a Tecnologia, I.P., under the projects with reference UIDB/00144/2020 and UIDP/00144/2020.

REFERENCES

- [1] M. Aguiar, P. Ashwin, A. Dias and M. Field. Dynamics of coupled cell networks: synchrony, heteroclinic cycles and inflation, *J. Nonlin. Sci.* **21** (2011) 271–323; doi:10.1007/s00332-010-9083-9.
- [2] M.A.D. Aguiar and A.P.S. Dias. Minimal coupled cell networks, *Nonlinearity* **20** (2007) 193–219; doi:10.1088/0951-7715/20/1/012.
- [3] M.A.D. Aguiar and A.P.S. Dias. Coupled cell networks: minimality, *Proc. Appl. Math. Mech.* **7** (2007) 1030501–1030502; doi:10.1002/pamm.200700991.
- [4] M. Aguiar, A. Dias, and H. Ruan. Synchrony patterns in gene regulatory networks, *Physica D: Nonlinear Phenomena* **429** (2022) 133065; doi:10.1016/j.physd.2021.133065.
- [5] M. Aguiar, A. Dias, and P. Soares. Towards a classification of networks with asymmetric inputs, *Nonlinearity* **34** (2021) 5630–5661; doi:10.1088/1361-6544/ac0b2e.
- [6] M. Aguiar, A. Dias, and I. Stewart. Classification of 3-node excitatory-inhibitory networks, in preparation.
- [7] F. Antoneli, M. Golubitsky, and I. Stewart. Homeostasis in a feed forward loop gene regulatory network motif, *J. Theoretical Biology* **445** (2018) 103–109; doi:10.1016/j.jtbi.2018.02.026.
- [8] M.R. Atkinson, M.A. Savageau, J.T. Myers, and A.J. Ninfa. Development of genetic circuitry exhibiting toggle switch or oscillatory behavior in *Escherichia coli*, *Cell* **113** (2003) 597–60; doi:10.1016/S0092-8674(03)00346-5.
- [9] P. Boldi and S. Vigna. Fibrations of graphs, *Discrete Math.* **243** (2002) 21–66; doi:10.1016/S0012-365X(00)00455-6.
- [10] E. Conrad, A.E. Mayo, A.J. Ninfa, and D.B. Forger. Rate constants rather than biochemical mechanism determine behaviour of genetic clocks, *J. R. Soc. Interface* **5** (2008) S9–S15; doi:10.1098/rsif.2008.0046.focus.
- [11] N. Dalchau, G. Szé, R. Hernansaiz-Ballesteros, C.P. Barnes, L. Cardelli, A. Phillips *et al.* Computing with biological switches and clocks, *Natural Computing* **17** (2018) 761–779; doi:10.1007/s11047-018-9686-x.
- [12] L. DeVille and E. Lerman. Modular dynamical systems on networks, *J. Eur. Math. Soc.* **17** (2013); doi:10.4171/JEMS/577.
- [13] A.P.S. Dias and I. Stewart. Linear Equivalence and ODE-equivalence for coupled cell networks, *Nonlinearity* **18** (2005) 1003–1020; doi:10.1088/0951-7715/18/3/004
- [14] M.B. Elowitz and S. Leibler. A synthetic oscillatory network of transcriptional regulators, *Nature* **403** (2000) 335–338; doi:10.1038/35002125.
- [15] M. Field. Combinatorial dynamics, *Dynamical Systems* **19** (2004) 217–243; doi:10.1080/14689360410001729379.
- [16] E. Fung, W.W. Wong, J.K. Suen, T. Bulter, S. Gu Lee, and J.C. Liao. A synthetic gene-metabolic oscillator, *Nature* **435** (2005) 118–122; doi:10.1038/nature03508.
- [17] S. Gama-Castro *et al.* RegulonDB version 9.0: high-level integration of gene regulation, co-expression, motif clustering and beyond, *Nucleic Acids Res.* **44** (2016) D133–D143.

- [18] T.S. Gardner, C.R. Cantor, and J.J. Collins. Construction of a genetic toggle switch in *Escherichia coli*, *Nature* **403** (2000) 339–42; doi:10.1038/3500213.
- [19] M. Golubitsky and I. Stewart. Nonlinear dynamics of networks: the groupoid formalism, *Bull. Amer. Math. Soc.* **43** (2006) (3) 305–364; doi:10.1090/S0273-0979-06-01108-6.
- [20] M. Golubitsky and I. Stewart. Homeostasis, singularities, and networks, *J. Math. Biol.* **1** (2016); doi:10.1007/s00285-016-1024-2.
- [21] M. Golubitsky and I. Stewart. Homeostasis with multiple inputs, *SIAM J. Appl. Dyn. Sys.* **17** (2018) 1816–1832; doi:10.1137/17M115147X.
- [22] M. Golubitsky and I. Stewart. *Dynamics and Bifurcation in Networks: Theory and Applications of Coupled Differential Equations*, SIAM, Philadelphia 2023; doi:10.1137/1.9781611977332.
- [23] M. Golubitsky, I. Stewart, F. Antoneli, Z. Huang, and Y. Wang. Input-output networks, singularity theory, and homeostasis, in: *Advances in Dynamics, Optimization and Computation* (eds. O. Junge, O. Schütze, G. Froyland, S. Ober-Blöbaum, and K. Padberg-Gehle), Studies in Systems, Decision and Control **304**, Springer, Berlin 2020, 31–65.
- [24] M. Golubitsky, I. Stewart, and A. Török. Patterns of synchrony in coupled cell networks with multiple arrows, *SIAM J. Appl. Dyn. Sys.* **4** (2005) 78–100; doi:10.1137/0406126.
- [25] M. Golubitsky and Y. Wang. Infinitesimal homeostasis in three-node input-output networks, *J. Math. Biol.* **80** (2020) 1163–1185; doi:10.1007/s00285-019-01457-x.
- [26] B.C. Goodwin. *Temporal Organization in Cells: a Dynamic Theory of Cellular Control Processes*, Academic Press, London 1963.
- [27] C.L. Grove and R.P. Gunsalus. Regulation of the *aroH* operon of *Escherichia coli* by the tryptophan repressor, *J. Bacteriol.* **169** (1987) 21582164.
- [28] R. Guantes and J.F. Poyatos. Dynamical principles of two-component genetic oscillators, *PLoS Comput. Biol.* **2** (2006) e30; doi:10.1371/journal.pcbi.0020030.
- [29] P. Hagmann. *From Diffusion MRI to Brain Connectomics*, Thesis, EPFL Lausanne 2005. doi:10.5075/epfl-thesis-3230.
- [30] J. Hasty, M. Dolnik, V. Rottschäfer, and J.J. Collins. Synthetic gene network for entraining and amplifying cellular oscillations, *Phys. Rev. Lett.* **88** (2002) 148101; doi:10.1103/PhysRevLett.88.148101.
- [31] J. Hasty, F. Isaacs, M. Dolnik, D. McMillen, and J.J. Collins. Designer gene networks: towards fundamental cellular control, *Chaos* **11** (2001) 207–220; doi:10.1063/1.1345702.
- [32] H. Kamei. Construction of lattices of balanced equivalence relations for regular homogeneous networks using lattice generators and lattice indices, *Internat. J. Bif. Chaos* **19** (2009) 3691–3705; doi:10.1142/S0218127409025067.
- [33] B.P. Kramer and M. Fussenegger. Hysteresis in a synthetic mammalian gene network, *Proc. Natl. Acad. Sci. USA* **102** (2005) 9517–9522; doi:10.1073/pnas.0500345102.
- [34] B.P. Kramer, A.U. Viretta, M.D.-E. Baba, D. Aube, W. Weber, and M. Fussenegger. An engineered epigenetic transgene switch in mammalian cells, *Nature Biotech.* **22** (2004) 867–870; doi:10.1038/nbt980.
- [35] Y. Kuramoto. Self-entrainment of a population of coupled non-linear oscillators, in: *International Symposium on Mathematical Problems in Theoretical Physics* (ed. H. Araki), Lect. Notes in Physics **39**, Springer, New York 1975, 420–422.
- [36] Y. Kuramoto. *Chemical Oscillations, Waves, and Turbulence*, Springer, Berlin 1984.
- [37] I. Leifer, F. Morone, S.D.S. Reis, J.S. Andrade Jr., M. Sigman, and H.A. Makse. Circuits with broken fibration symmetries perform core logic computations in biological networks, *PLOS Computational Biology* (2020); doi:10.1371/journal.pcbi.1007776 0.

- [38] M.C.A. Leite and M. Golubitsky. Homogeneous three-cell networks, *Nonlinearity* **19** (2006) 2313–2363; doi:10.1088/0951-7715/19/10/004.
- [39] E. Liu, L. Li, L. Cheng. Gene regulatory network review, in: *Encyclopedia of Bioinformatics and Computational Biology* (eds. S. Ranganathan, M.I. Gribskov, K. Nakai, and C. Schönbach), Academic Press New York 2019, 155–164.
- [40] H.A. Makse, Genetic circuits, preprint 2020.
- [41] H.A. Makse, M. Golubitsky, H.S. Monteiro, S.D.S. Reis, and I. Stewart. Dynamics and bifurcations in genetic circuits with fibration symmetries, in preparation 2023.
- [42] H.A. Makse, I. Stewart, P. Boldi, and F. Sorrentino. *Symmetries of Living Systems: Graph Fibrations and Cluster Synchronization in Biological Networks*, Cambridge University Press, to appear.
- [43] R. Milo, S. Shen-Orr, S. Itzkovitz, N. Kashtan, D. Chklovskii, and U. Alon. Network motifs: simple building blocks of complex networks, *Science* **298** (2002) 824–827; doi:10.1126/science.298.5594.824.
- [44] F. Morone, I. Leifer, and H.A. Makse. Fibration symmetries uncover the building blocks of biological networks, *Proc. Nat. Acad. Sci. USA* **117** (2020) 8306–8314; doi:10.1073/pnas.191462811.
- [45] F. Morone, and H.A. Makse. Network symmetries of living systems, preprint.
- [46] O. Purcell, N.J. Savery, C.S. Grierson, and M. di Bernardo. A comparative analysis of synthetic genetic oscillators, *J. Roy. Soc. Interface* **7** (2010) 1503–1524; doi:10.1098/rsif.2010.0183.
- [47] R. Singhania and J.J. Tyson. Evolutionary Stability of Small Molecular Regulatory Networks That Exhibit Near-Perfect Adaptation, *Biology (Basel)* **12** (6) (2023) 841; doi: 10.3390/biology12060841.
- [48] P. Smolen, D.A. Baxter, and J.H. Byrne. Frequency selectivity, multistability, and oscillations emerge from models of genetic regulatory systems, *Amer. J. Physiol.* **274** (1998) C531–C542; doi:10.1152/ajpcell.1998.274.2.C531
- [49] O. Sporns, G. Tononi, and R. Kötter. The human connectome: a structural description of the human brain, *PLOS Computational Biology* **1** (2005) e42; doi:10.1371/journal.pcbi.0010042.
- [50] I. Stewart, M. Golubitsky and M. Pivato. Symmetry groupoids and patterns of synchrony in coupled cell networks, *SIAM J. Appl. Dynam. Sys.* **2** (2003) 609–646; doi:10.1137/S1111111103419896.
- [51] M. Tigges, T.T. Marquez-Lago, J. Stelling, and M. Fussenegger. A tunable synthetic mammalian oscillator, *Nature* **457** (2009) 309–312; doi:10.1038/nature07616.
- [52] J.J. Tyson and B. Novák. Functional motifs in biochemical reaction networks, *Ann. Rev. Phys. Chem.* **61** (2010) 219–240; doi:10.1146/annurev.physchem.012809.103457.

MANUELA AGUIAR, CENTRO DE MATEMÁTICA DA UNIVERSIDADE DO PORTO (CMUP), FACULDADE DE CIÊNCIAS, UNIVERSIDADE DO PORTO, RUA DO CAMPO ALEGRE S/N, 4169-007 PORTO, PORTUGAL

FACULDADE DE ECONOMIA, UNIVERSIDADE DO PORTO, RUA DR ROBERTO FRIAS, 4200-464 PORTO, PORTUGAL

Email address: `maguiar@fep.up.pt`

ANA DIAS, CENTRO DE MATEMÁTICA DA UNIVERSIDADE DO PORTO (CMUP), DEPARTAMENTO DE MATEMÁTICA, FACULDADE DE CIÊNCIAS, UNIVERSIDADE DO PORTO, RUA DO CAMPO ALEGRE S/N, 4169-007 PORTO, PORTUGAL

Email address: `apdias@fc.up.pt`

IAN STEWART, MATHEMATICS INSTITUTE, UNIVERSITY OF WARWICK, COVENTRY CV4 7AL, UNITED KINGDOM

Email address: `i.n.stewart@warwick.ac.uk`